

University of Central Florida

**STARS**

---

Electronic Theses and Dissertations

---

2005

## Correlation Of Acoustic Emission Parameters With Weight And Velocity Of Moving Vehicles

Amar Kolgaonkar

*University of Central Florida*



Part of the [Mechanical Engineering Commons](#)

Find similar works at: <https://stars.library.ucf.edu/etd>

University of Central Florida Libraries <http://library.ucf.edu>

This Masters Thesis (Open Access) is brought to you for free and open access by STARS. It has been accepted for inclusion in Electronic Theses and Dissertations by an authorized administrator of STARS. For more information, please contact [STARS@ucf.edu](mailto:STARS@ucf.edu).

---

### STARS Citation

Kolgaonkar, Amar, "Correlation Of Acoustic Emission Parameters With Weight And Velocity Of Moving Vehicles" (2005). *Electronic Theses and Dissertations*. 344.

<https://stars.library.ucf.edu/etd/344>

CORRELATION OF ACOUSTIC EMISSION PARAMETERS WITH WEIGHT AND  
VELOCITY OF MOVING VEHICLES

by

AMAR D. KOLGAONKAR  
B.S. University of Pune, 2000

A thesis submitted in partial fulfillment of the requirements  
for the degree of Master of Science  
in the Department of Mechanical, Materials and Aerospace Engineering  
in the College of Engineering and Computer Science  
at the University of Central Florida  
Orlando, Florida

Spring Term  
2005

© 2005 Amar Kolgaonkar

## **ABSTRACT**

The thesis is motivated by the goal of doing initial investigation and experimentation for the development of Weigh-in-Motion (WIM) system using acoustic emission phenomenon. A great deal of research is going on for measuring the weight of moving vehicles. Weigh-in-motion of commercial vehicles is essential for management of freight traffic, highway infrastructure design and maintenance, and monitoring of heavy weight vehicles.

The research work presents a methodology for correlating the weight of a moving vehicle with acoustic emission parameters (such as counts and energy). Furthermore, the correlation between the speed of vehicle with the acoustic emission parameters is developed. Preliminary analysis and experimentations were conducted for the study of propagation of acoustic signals in plate like structure and effect of dynamic loadings on Kaiser Effect.

Initial testing revealed that there is a linear correlation between the impact force and the acoustic emission parameters. Also a polynomial regression of second order was found between the speed of vehicle and acoustic emission parameters. Road testing was conducted to investigate the correlation between weight of the vehicle and acoustic emission parameters. A linear relation was found between the weight of vehicle and acoustic emission parameters represented by counts, signal energy and absolute energy.

## **ACKNOWLEDGMENTS**

I would like to extend special thanks to Dr. Faissal Moslehy, my committee chair for his encouragement, valuable guidance and support throughout my research. I would like to express my appreciation towards the members of my committee, Dr. David Nicholson and Dr. Amr Oloufa for their assistance and cooperation. I would like to thank all my friends for their valuable and unyielding support throughout the completion of my thesis. Finally, I would like to thank my family for their wisdom, support and understanding throughout the period of my study.

# TABLE OF CONTENTS

LIST OF FIGURES .....	vii
LIST OF TABLES .....	xi
CHAPTER ONE: INTRODUCTION.....	1
CHAPTER TWO: LITERATURE REVIEW.....	5
2.1 ASTM Classification .....	6
2.2 Bending Plate System .....	8
2.3 Piezoelectric System .....	10
2.4 Load Cell System.....	12
2.5 Cost Comparison of different WIM Systems.....	14
2.6 Accuracy of WIM Systems.....	15
2.7 Acoustic Emission .....	16
CHAPTER THREE: ACOUSTIC EMISSION MONITORING.....	18
3.1 Terminology.....	18
3.2 Acoustic Emission Testing .....	23
3.2.1 <i>Conventional Acoustic Emission Monitoring</i> .....	23
3.2.2 <i>Quantitative Acoustic Emission Testing</i> .....	24
3.3 Instrumentation .....	25
3.3.1 <i>System Hardware</i> .....	25
3.3.2 <i>System Software</i> .....	26
3.3.3 <i>AE Data Display</i> .....	27
3.4 Lamb Waves .....	30

CHAPTER FOUR: METHODOLOGY .....	34
4.1 AE Calibration Test .....	34
4.2 Frequency Bandwidth Selection .....	38
4.3 Material Selection for the Strip.....	39
4.4 Kaiser Effect due to Impact Force .....	39
4.5 Variable Impact Force.....	46
CHAPTER FIVE: TESTING AND RESULTS.....	52
5.1 Bike Test .....	52
5.2 Car Road Test .....	54
5.2.1 <i>Car Test with Varying Speed</i> .....	54
5.2.2 <i>Car Test with Varying Weight</i> .....	63
CHAPTER SIX: CONCLUSIONS .....	76
LIST OF REFERENCES .....	77

## LIST OF FIGURES

Figure 2.1: Example of Bending Plate WIM System Layout. ....	9
Figure 2.2: Example of Piezoelectric WIM System Layout. ....	11
Figure 2.3: Example Layout for the Load Cell WIM system. ....	13
Figure 3.1: Schematic representation of Acoustic emission monitoring. ....	19
Figure 3.2: Typical Acoustic Emission Signal. ....	22
Figure 3.3: Phase velocity dispersion curves for aluminum plate. ....	31
Figure 3.4: Group velocity dispersion curve for aluminum plate. ....	31
Figure 3.5: AE Signals produced due to low velocity impact on plate. ....	33
Figure 3.6: AE Signals produced due to high velocity impact on plate. ....	33
Figure 4.1: Schematic representation of pencil lead break test to calculate velocity. ....	36
Figure 4.2: Plot of Events Vs Position for Test. ....	37
Figure 4.3: A typical signal produced by pencil lead break on the surface of strip. ....	37
Figure 4.4: Schematic representation of the test for monitoring Kaiser Effect. ....	41
Figure 4.5: A signal generated due to impact force on aluminum strip. ....	42
Figure 4.6: Variation of AE Counts for 10 trials collected by Channel-1. ....	44
Figure 4.7: Variation of AE Counts for 10 trials collected by Channel-2. ....	44
Figure 4.8: Variation of Signal Energy for 10 Trials collected by Channel-1. ....	45
Figure 4.9: Variation of Signal Energy for 10 Trials collected by Channel-2. ....	45
Figure 4.10: Schematic representation of Variable impact test on aluminum strip. ....	47
Figure 4.11: Variation of counts w.r.t. impact energy for signals acquired through channel-1. ....	49



Figure 4.12: Variation of counts w.r.t. impact energy for signals acquired through	49
channel-2.....	49
Figure 4.13: Variation of signal energy w.r.t. impact energy for signals acquired through	
channel-1.....	50
Figure 4.14: Variation of signal energy w.r.t. impact energy for signals acquired through	
channel-2.....	50
Figure 4.15: Variation of absolute energy w.r.t. impact energy for signals acquired	
through channel-1. ....	51
Figure 4.16: Variation of absolute energy w.r.t. impact energy for signals acquired	
through channel-2. ....	51
Figure 5.1: Schematic Representation of Bike test. ....	53
Figure 5.2: Aluminum and Steel strip attached to ground. ....	55
Figure 5.3: Test setup during the car test. ....	55
Figure 5.4: Schematic Representation of Car Test. ....	57
Figure 5.5: Car test being conducted .....	57
Figure 5.6: Variation of AE Counts w.r.t Speed of vehicle when front wheel passes over	
the strip.....	60
Figure 5.7: Variation of AE Counts w.r.t Speed of vehicle when rear wheel passes over	
the strip.....	60
Figure 5.8: Variation of Signal Energy w.r.t. Speed of vehicle when front wheel passes	
over the strip. ....	61
Figure 5.9: Variation of Signal Energy w.r.t. Speed of Vehicle when rear wheel passes	
over the strip. ....	61

Figure 5.10: Variation of Absolute Energy w.r.t. Speed of Vehicle when front wheel passes over the strip. ....	62
Figure 5.10: Variation of Absolute Energy w.r.t. Speed of Vehicle when front wheel passes over the strip. ....	62
Figure 5.11: Variation of Absolute Energy w.r.t Speed of Vehicle when rear wheel passes over the strip. ....	62
Figure 5.12: Variation of counts w.r.t weight in vehicle when front wheel passes over the strip. ....	65
Figure 5.13: Variation of counts w.r.t. weight in vehicle when rear wheel passes over the strip. ....	65
Figure 5.14: Variation of signal energy w.r.t weight in vehicle when front wheel passes over the strip. ....	66
Figure 5.15: Variation of signal energy w.r.t weight in vehicle when rear wheel passes over the strip. ....	66
Figure 5.16: Variation of absolute energy w.r.t. weight in vehicle when front wheel passes over the strip. ....	67
Figure 5.17: Variation of absolute energy w.r.t. weight in vehicle when rear wheel passes over the strip. ....	67
Figure 5.18: Signal acquired by data acquisition card. ....	70
Figure 5.19: Linear frequency domain plot for the acquired signal. ....	70
Figure 5.20: Logarithmic frequency domain plot for the acquired signal. ....	71
Figure 5.21: 2D plot of wavelet coefficients. ....	71
Figure 5.22: 3D plot of wavelet coefficient. ....	72

Figure 5.23: Variation of wavelet coefficient w.r.t. impact energy..... 72

Figure 5.24: Surface plot for Counts with variation of speed and weight with in the Car75

Figure 5.25: Surface plot for Energy with variation of speed and weight with in the Car75

## LIST OF TABLES

Table 2.1: ASTM Weigh-in-Motion System Types. ....	7
Table 2.2: Cost comparison of WIM Systems. ....	14
Table 2.3: Comparison of weigh-in-motion systems. ....	15
Table 2.4: Tolerances of different WIM systems. ....	16
Table 4.1: AE parameters acquired by channel-1 when constant impact force is applied for 10 trials. ....	43
Table 4.2: AE parameters acquired by channel-2 when constant impact force is applied for 10 trials. ....	43
Table 4.3: AE parameters acquired by channel-1 when variable impact force was applied. .....	48
Table 5.1 Acoustic emission parameters acquired during bike test. ....	53
Table 5.2: AE results when front wheel passes over the strip. ....	59
Table 5.3: AE results when rear wheel passes over the strip. ....	59
Table 5.4: Acoustic emission parameters acquired when front wheel passes over the strip. .....	64
Table 5.5: Acoustic emission parameters acquired when rear wheel passes over the strip. .....	64
Table 5.6: 3-dimensional chart with acoustic emission parameters as input for particular speed and weight of vehicle. ....	73
Table 5.7: Variation of Counts with the speed and weight with in the car. ....	74
Table 5.8: Variation of Energy with the speed and weight with in the car. ....	74

## **CHAPTER ONE: INTRODUCTION**

Transportation infrastructure has always been a lifeline for any nation, as it contributes to the economic prosperity and social well being. An efficient and safe road network is very much essential which cannot be neglected and stringent steps must be taken to ensure that the highway system meets all the safely requirements and is useable. An efficient and safe highway network allows goods to be transported safely, thus stimulating economic activity and ensuring trade competitiveness. A safe and efficient highway network helps motorists to travel with ease, have less frustration, and spend or save more time for other activities. “In USA, over 46,000 miles of interstate highways combined with a network of almost 4 million miles of other roads makes up the nation’s lifeline.”<sup>1</sup> Every year nearly five trillion dollars worth of goods are transported through commercial trucks<sup>2</sup> with increase in every year. However commercial trucks are responsible for deteriorating the highway infrastructure and making them unsafe for travel.

Heavy or overloaded commercial vehicles are potential hazards for highway infrastructures, mainly the bridges. Each overloaded vehicle adds a certain amount of damage to the highways. It was found that increase in load causes four times the increase in acceleration of pavement wear. That is, if a pavement is subjected to 10% overloading then the acceleration of pavement wear would be 45%.<sup>3</sup> Thus, higher overload and more often it happens, means shorter pavement life and more frequent maintenance is required. Hence strict weight enforcement is necessary to minimize the pavement wear and the cost attributed to it. Truck weight regulations are in place to protect pavements and bridges

form the effects of overloaded vehicles, to maintain manageable traffic conditions and to ensure safety on highways. The first law for truck weight regulation was passed in the year 1913, and by 1933, all states had some kind of truck weight limit.<sup>4</sup> Transport Research Board states “enforcement is a critical plan for vehicle weights, which includes certainty of penalties and sanctions sufficient to deter violations, without which, weight limit laws would become meaningless”.<sup>5</sup> Enforcements are intended to balance the economic benefits of commercial vehicle operation with the various costs resulting from pavement maintenance cost, new construction cost, public safety, and additional design requirements for the infrastructure.

Traditionally weigh stations with static scales were used to weigh majority of commercial vehicles on road. Static weigh stations are advantageous when there is low truck intensity. However, in most of the cases, the static weigh stations can not accommodate existing or projected truck volumes. Also at traditional weigh stations all the trucks are required to report for visual inspection and static weighing. At the busier weigh stations the trucks are queued on the ramps before they are passed over the weigh scales. As the queue extends from ramps to highway lanes they tend to obstruct normal flow of traffic, causing safety hazard of having immobile trucks adjacent to vehicles traveling in excess of 50 miles per hour. Sometimes the weigh stations are closed down temporary till the queue diminishes. However when the weigh stations are closed, some trucks are able to bypass the weighing process and continue to travel on highways even though they might be overweight, causing damage to highway infrastructure.

Delays are caused to the trucker when weigh stations are closed or when they have to stay in queue for a long time. Over a period of time, the number of delays to

truckers might translate into an enormous economic loss to trucking industry. Hence there is a need to eliminate unnecessary delays for truckers while also accomplishing the enforcement laws.

For many years now transportation researchers are looking for a system that can help to protect the highway infrastructure, reduce pavement maintenance cost and ensure public safety. Weigh-in-Motion (WIM) technology provides solution to everyone involved in highway maintenance and safety. In past several years, many countries are using Weigh-in-Motion (WIM) technology to reduce delay and increase enforcement for overweight vehicles. Weigh in motion is defined by the American Society for Testing and Materials (ASTM) as “The process of estimating a moving vehicle’s gross weight and a portion of that weight that is carried by each wheel, axle, or axle group, or combination thereof, by measurement and analysis of dynamic vehicle tire forces”.

Highway management activities include the weighing of vehicles to protect existing infrastructure and the collection of traffic data to plan for further investments in highway infrastructure. Thus WIM serves two important functions,

- Enforcement for overloaded commercial vehicles to prevent deterioration of highway infrastructure.
- Collects data for further planning of highway infrastructure.

For weight enforcement purpose, weigh-in-motion is used to complement the existing static weighing activities at weighing stations. As known, static weigh station cannot handle the volume of trucks passing through weigh station so WIM acts as added equipment to existing weigh stations and makes them more efficient. WIM scale, automatically measures weight of all the trucks traveling at highway speed and sorts them

depending upon their weight. Based on a pre-clearance criteria determined by the state law, trucks which are suspected to be overweight are directed to the static weigh scale for more accurate measurement while the others are allowed to bypass the static scale with minimum interruption. WIM has become a valuable enforcement tool for targeting potential violators thus allowing legal operators to benefit tremendously from fewer interruptions to their operation. WIM effectively helps to discriminate between the good carriers and those who attempt to operate outside the law to gain a price advantage.

For data collection purpose, WIM system installed on the main lane continuously collects the valuable data such as truck weight, speed, time of travel and axle configuration at all the times even when the regular truck weighing stations are closed. This is very helpful because the number of overweight trucks rises when the weigh stations are known to be closed. Drivers of overweight vehicles tend to pass by the weigh station when they are closed or tend to choose an alternate route. For example in California<sup>6</sup> it is found that immediately after modifying the regular enforcement hours, there was higher incidence of overweight violation. When WIM system is installed, overweight trucks cannot avoid detection thus tendency to travel when weigh stations are closed is reduced. WIM also gives valuable traffic loading data which helps the highway department to plan maintenance activities to have prolonged integrity of a road. Maintenance activities can be mis-timed due to incorrect traffic loading data which would lead to deterioration of roads. WIM system provides traffic information data which is used by the state department for management, evaluation and planning purposes.



## **CHAPTER TWO: LITERATURE REVIEW**

The weight of trucks and other cargo carrying vehicles decides the design of highway infrastructure such as roads and bridges. To maintain the highway infrastructure, weight limit requirements are imposed almost everywhere. For the past several years, many countries are using Weigh-in-Motion (WIM) technology to reduce delays and increase enforcement of overweight vehicles. Weigh-in-motion is defined by the American Society for Testing and Materials (ASTM) as “The process of estimating a moving vehicle’s gross weight and a portion of that weight that is carried by each wheel, axle, or axle group, or combination thereof, by measurement and analysis of dynamic vehicle tire forces”. With the help of weigh-in-motion technology trucks can be weighed dynamically and henceforth depending upon the weight recorded, can be indicated to continue or to enter a static scale for more accurate measurements.

Weigh-in-motion has improved and made the operation of weigh stations, very much convenient and comfortable. There are various types of WIM scales with different accuracy levels. As the accuracy level of weigh-in-motion system decreases the number of trucks entering the static scale for accurate measurement, increases. Also if the weigh –in-motion system underestimates a vehicle’s weight, overloaded trucks potentially pass through the system without being stopped and may accelerate the degradation of highways and bridges.

The literature review encompasses analysis of various technical papers, standards set by the American Society of Testing Materials, various types of weigh-in-motion systems, accuracy of weigh-in-motion systems and calibration techniques. Literature

review helps to understand the strengths and shortcomings of weigh-in-motion technology.

## **2.1 ASTM Classification**

Weigh-in-motion systems are classified into four different types according to ASTM specification E 1318-94 (ASTM 1994). The classification of weigh-in-motion system depends upon, speed of the vehicle, type of application and other desired characteristics. Table 2.1 gives the basic difference between each ASTM type<sup>7</sup> (McCall *et al.*, 1997). ASTM Type I and Type II are used for traffic data collection and are used in up to four lanes of travel. ASTM Type III and Type IV weigh-in-motion systems are used for weight enforcement and are used in up to two lanes of travel (McCall *et al.*, 1997 and ASTM, 1997). ASTM also defines weigh-in-motion as a set of sensors and supporting instruments which measures presence of vehicle, estimates tire loads, speed, axle spacing, vehicle class according to axle spacing and other parameters related to vehicle; processes, and stores this information.

Instrumentation for weigh-in-motion is divided into different parts<sup>8</sup> (Laurita *et al.*, 1994). It includes detectors to check the presence and measurement of vehicle speed, a WIM scale and a height detector. The computer components consist of desktop computer, display, modem, and printer. The signalization components consist of directional signals and variable message signs.

Table 2.1: ASTM Weigh-in-Motion System Types.

	CLASSIFICATION			
	Type I	Type II	Type III	Type IV
Speed Range	10-70 mph	10-70 mph	15-50 mph	0-10 mph
Application	Traffic data collection	Traffic data collection	Weight Enforcement	Weight Enforcement
Number of Lanes	Upto 4	Upto 4	Upto 2	Upto 2
Bending Plate	X	X	X	X
Piezoelectric Sensor	X	X		
Load Cell	X	X	X	X
Wheel Load	X		X	X
Axle Load	X	X	X	X
Gross Vehicle Load	X	X	X	X
Speed	X	X	X	X
Center-to-Center Axle Spacing	X	X	X	X
Vehicle Class	X	X		
Site Identification Code	X	X	X	X
Lane and Direction of Travel	X	X	X	
Date and Time of Passage	X	X	X	X
Sequential Vehicle Record Number	X	X	X	X
Wheel Base	X	X		
Equivalent Single-Axle Load	X	X		
Violation Code	X	X	X	X

Source: FHWA "States Successful Practices Weigh-in-Motion Handbook" and ASTM E 1318

## **2.2 Bending Plate System**

In bending plate weigh-in-motion, strain gauges are bonded to the underside of plate (McCall et al., 1997). There are two types of bending plate systems, portable and permanent, depending upon the application. As the vehicle passes over the bending plate, the system records the strain measured through strain gauges and calculates the dynamic load. The static load is estimated from the measured strain and a calibration constant or parameter. Many factors are taken in to consideration by the calibration constant such as vehicle speed, vehicle dynamics and pavement dynamics. Depending upon the usage, bending plate system can also be classified as ASTM Type I, II, III, and IV.

Bending plate systems may have one or two scales in the travel lane placed perpendicular to the direction of travel.<sup>9</sup> Whenever two scales are used in a bending plate system, each scale is used for a single wheel path. The scales are placed side-by-side or at a particular distance away from each other. Inductive loops are placed upstream and downstream of the scale to measure the presence of vehicle and to determine the speed of passing vehicle. Data collection is done with the help of specific hardware and is processed with the help of software. A report is saved in an output file and is transferred through a physical download or to a control room with the help of modem. An example of Bending Plate system layout is shown in Figure 2.1.

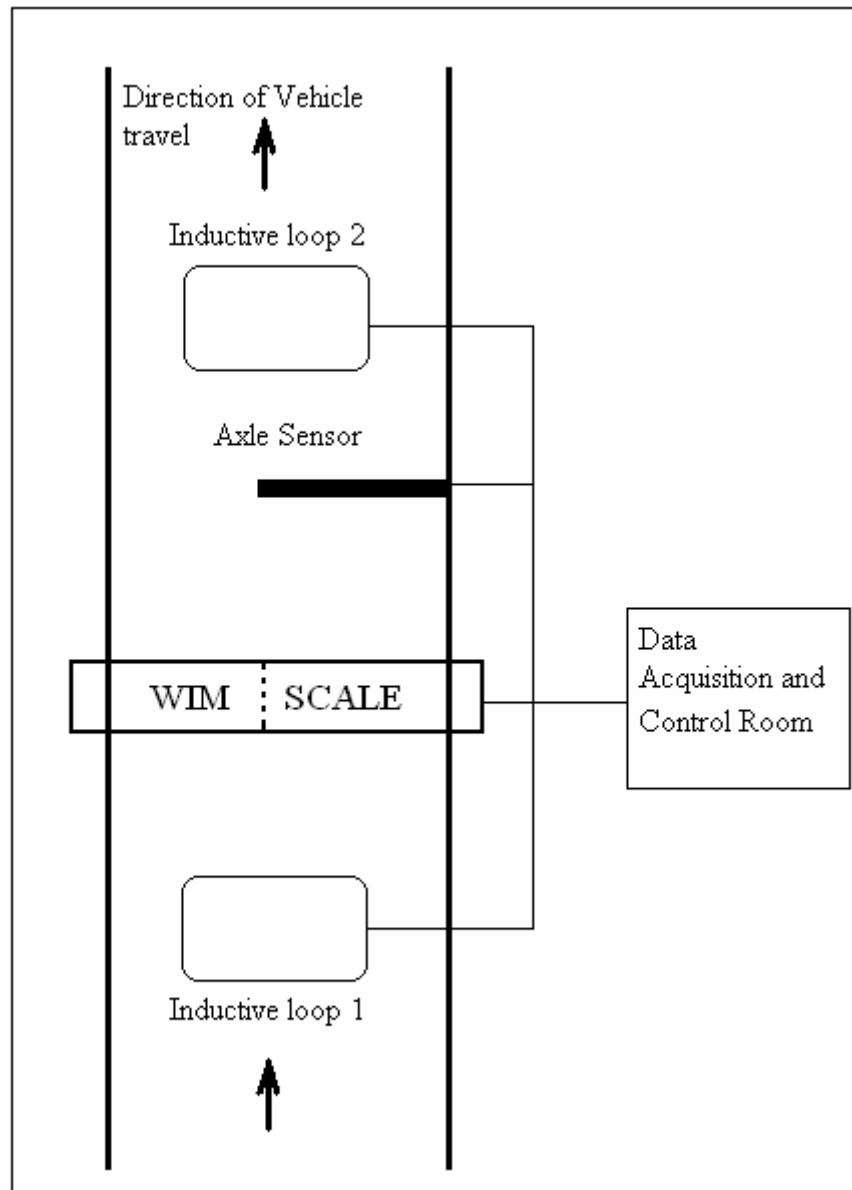


Figure 2.1: Example of Bending Plate WIM System Layout.

### **2.3 Piezoelectric System**

Piezoelectric weigh-in-motion system uses piezo sensors to measure the change in voltage caused due to pressure exerted by the moving vehicles on the sensor. As the vehicle passes over piezoelectric scale, the system measures the electrical charge generated by piezoelectric sensor and calculates dynamic load. Static load is calculated from dynamic load and the calibration parameters or constants. This system is classified as ASTM Type I or II depending upon their use and the number of sensors.

A typical piezoelectric WIM system consists of at-least one sensor and one inductive loop. Piezoelectric sensors are placed perpendicular to the direction of vehicle motion. The sensors span across the road so that both tires ride over the sensors. Similar to bending plate WIM, inductive loops are placed upstream and downstream of the sensors. The function of upstream sensors is to detect upcoming vehicle and alert the system, while downstream inductive loops are used for determination of vehicle speed and axle spacing. Again the information obtained from sensors, hardware and software can be stored or can be transferred through a modem connection. An example of piezoelectric WIM system layout is shown in Figure 2.2.

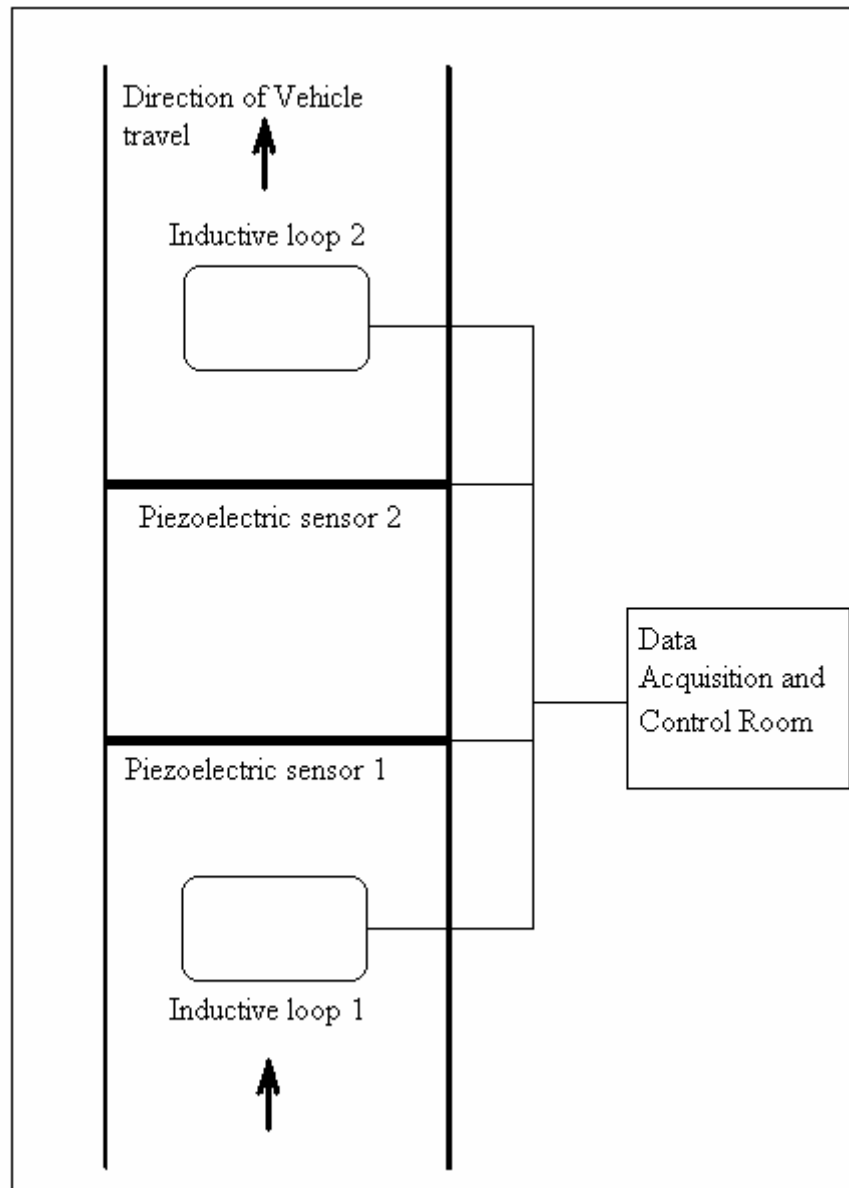


Figure 2.2: Example of Piezoelectric WIM System Layout.

## **2.4 Load Cell System**

Load cell WIM system has a single load cell with two scales to weigh both, the right and left part of axle simultaneously. As the vehicle passes over the load cell, weight is recorded by each scale and is added by the program to obtain total axle weight. It is classified depending upon the design of system as ASTM Type I, II, III, or IV.

The load scale is place in the travel lane and perpendicular to the direction of vehicle motion. A single inductive loop is placed upstream to detect any vehicle presence. If a second inductive loop is used then it is placed downstream to determine axle spacing, which is helpful in calculating the speed of the vehicle. A typical layout for load cell system is shown in Figure 2.3.



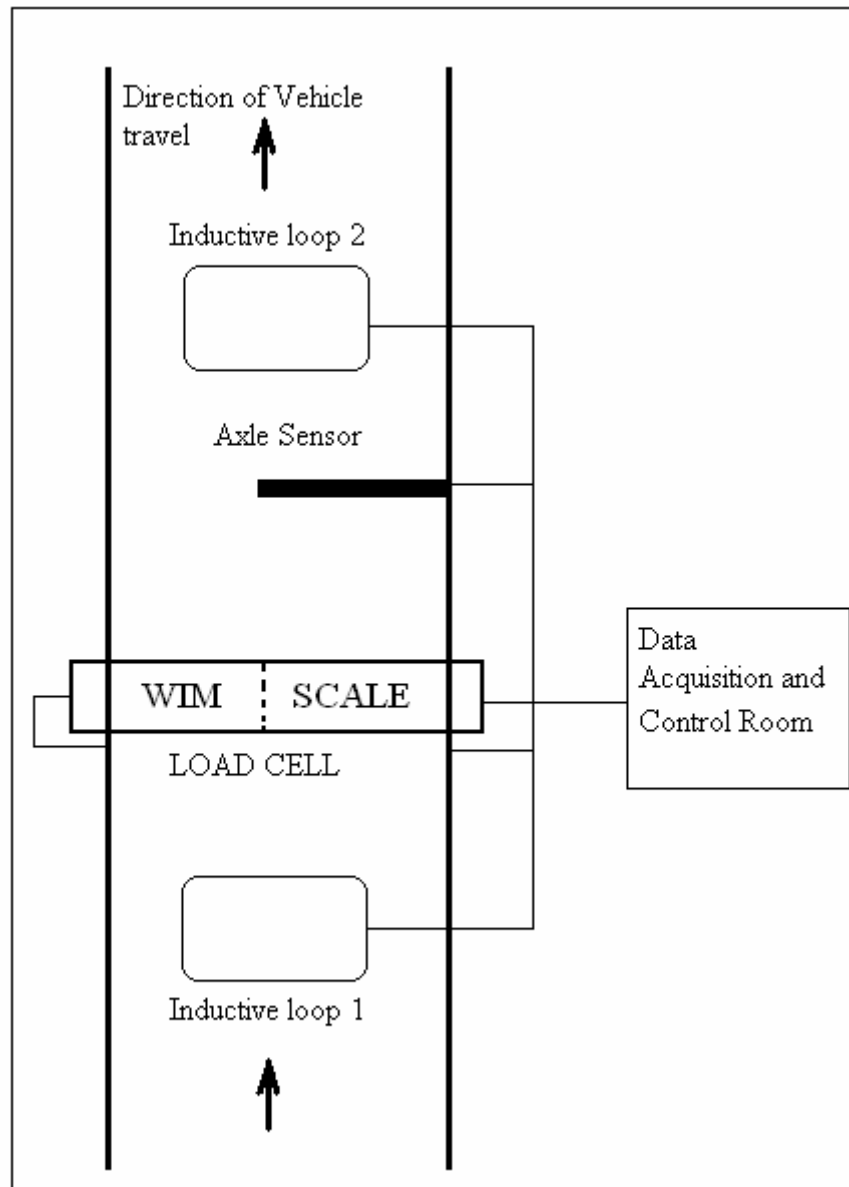


Figure 2.3: Example Layout for the Load Cell WIM system.

## 2.5 Cost Comparison of different WIM Systems

WIM systems provide different levels of accuracy at different system costs. Table 2.2 shows the economic analysis done by Taylor.<sup>10</sup> The costs shown for each system includes the estimated initial cost per lane and estimated average cost per lane. The estimated initial cost per lane includes the cost for equipment and installation. The performance of the system is calculated as percentage error on gross vehicle weight, whereas estimated average cost per lane is based on a life span of 12 years and includes maintenance cost.

Table 2.2: Cost comparison of WIM Systems.

WIM System	Performance	Estimated Initial Cost per Lane	Estimated Average Cost per Lane
Piezoelectric Sensor	10%	\$9,500	\$4,224
Bending Plate Scale	5%	\$18,900	\$4,990
Double Bending Plate Scale	3%-5%	\$35,700	\$7,709
Deep Pit Load Cell	3%	\$52,500	\$7,296

Bushman and Pratt<sup>11</sup> compared the three WIM technologies based on accuracy, life span and cost. The results were summarized in Table 2.3. The study revealed that the piezoelectric systems are the least accurate of the three technologies and also offer a very low life span of 4 years. The study also found out that as the accuracy of the system increases, its cost increases. The most accurate system found among the three was single

load cell with 6% accuracy at a 95% confidence level and also offers a longest life span. However the single load cell has the highest initial cost among the three systems.

Table 2.3: Comparison of weigh-in-motion systems.

	Piezoelectric System	Bending Plate System	Single Load Cell System
Accuracy (95% confidence)	15%	10%	6%
Expected Life	4 Years	6 Years	12 Years
Initial Installation Cost	\$9,000	\$21,000	\$48,700
Annual Installation Cost	\$4,750	\$6,400	\$8,300

## 2.6 Accuracy of WIM Systems

The actual load applied by vehicle while in motion includes more than the static weight of vehicle. As vehicle travels, the dynamic load applied by vehicle changes significantly due to acceleration or deceleration, bouncing of vehicle, weight transfer or pavement-tire interaction. Hence combination all these factors is recorded by WIM system. Further, errors due to measuring instrumentation have to be taken into consideration. Therefore two identical vehicles of same weight will produce signals with different characteristics depending upon tire pressure, vehicle speed, road roughness and sensor characteristics.

Accuracy of any WIM system is defined as, closeness between the weights measured by the WIM system and estimated reference value (ASTM, 1997). ASTM gives accuracy limits to each WIM system as a standard to set. As shown in the Table 2.4,

Types I, II and III tolerances are given in terms of percentages of known value and for Type IV tolerance is given in terms of pounds over the actual weight.

Table 2.4: Tolerances of different WIM systems.

Function	Tolerance for 95% Probability of Conformity			
	Type I	Type II	Type III	Type IV
Wheel Load	25%		20%	250 (100)
Axle Load	20%	30%	15%	500 (200)
Axle-Group Load	15%	20%	10%	1200 (500)
Gross-vehicle Weight	10%	15%	6%	2500 (1100)
Speed	1mph (2km/h)			
Axle-Spacing	0.5 ft (150mm)			

Source: ASTM Designation E 1318

## 2.7 Acoustic Emission

Acoustic emission (AE) is defined as a phenomenon where transient elastic waves are generated by the rapid release of energy from localized sources within a material. There might be different source mechanisms which would generate acoustic emission signals within material. Elastic waves propagate through the solid material and are recorded by one or more sensors. AE analysis is used as nondestructive evaluation (NDE) technique in wide range of applications such as locating faults in pressure vessels or leakage in storage tanks and piping system, corrosion detection, global or local long term monitoring of civil engineering structures such as bridges, offshore platforms etc. The disadvantage of acoustic emission is that it can only estimate qualitatively how much damage is caused with-in the material and approximately how long the component will

last. So, other NDE methods are still required to do more thorough examination and provide quantitative results. More detailed description about acoustic emission monitoring is explained further in a separate chapter.

## **CHAPTER THREE: ACOUSTIC EMISSION MONITORING**

Acoustic emission is a natural phenomenon occurring in a wide range of materials and structures. The large scale acoustic emissions are the seismic events, while the smallest possible scale processes observed are the movements of small number of dislocations in stressed metals. AE analysis is used in a wide range of applications such as detecting and locating faults in pressure vessels or leakage in storage tanks, monitoring welding applications, corrosion processes, fiber fracture or delamination and crack propagation. Figure 3.1 shows the schematic representation of acoustic emission process.

### **3.1 Terminology**

Acoustic emission (AE) is defined as a phenomenon where an elastic wave, in the range of ultrasound, usually 20 kHz to 1 MHz, is generated by rapid release of energy from the source within the material. A typical acoustic emission waveform is shown in Figure 3.2.

Signal is the electrical signal coming from transducer and passing through many signal conditioning equipments such as amplifiers, frequency filters etc.

Sensor is a device which contains a transducer element that turns AE wave motion into an electrical voltage.

Channel is a single AE sensor and related equipment components for transmitting, conditioning, detecting and measuring the signals that come from it.

Count is the number of times the AE signal crosses the detection threshold, also known as “ringdown counts” or “threshold crossing counts”.

Event is the local material change giving rise to acoustic emission.

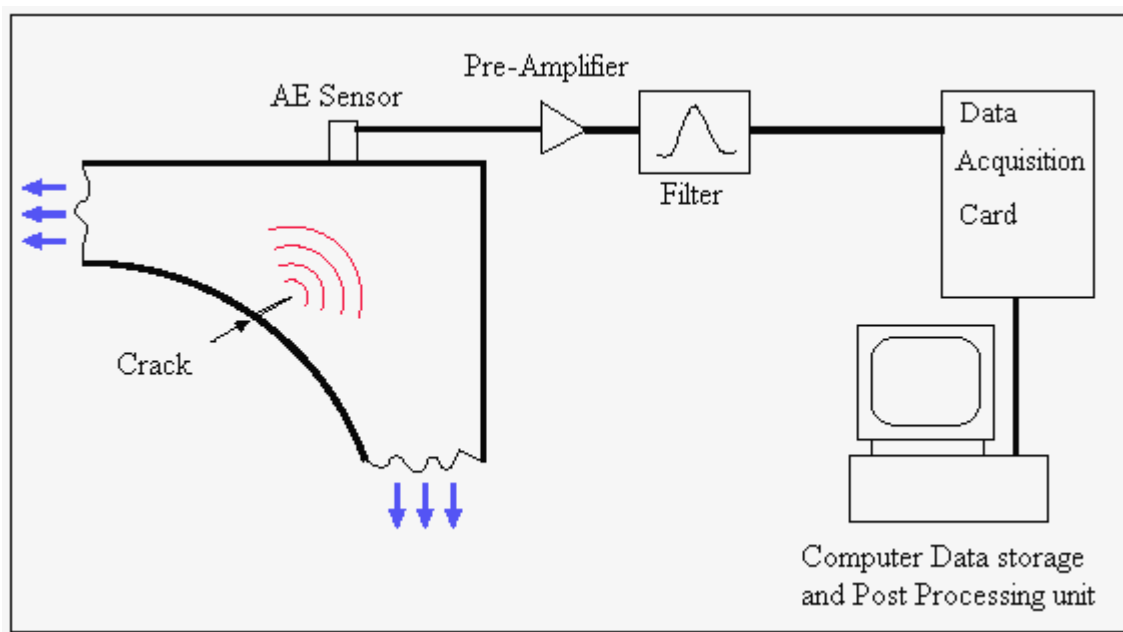


Figure 3.1: Schematic representation of Acoustic emission monitoring.

Hit is detection and measurement of an AE signal on a channel.

Amplitude is the peak voltage in the AE signal waveform. It is expressed in decibels relative to 1 microvolt at the pre-amplifier input (dB) assuming a 40 dB preamp. For example 0 dB corresponds to a 100  $\mu$ volt peak at the output of 40 dB preamplifier and 100 dB would correspond to a 10 volt peak signal at the output of the preamplifier.

Rise Time is defined as the time between the start of AE hit and the peak amplitude of an AE signal.

Duration is defined as the time from the first threshold crossing to the end of the last threshold crossing of the AE signal from the AE threshold.

Signal Strength is defined as “integral of the rectified voltage signal over the duration of AE waveform.”

Energy also known as PAC Energy<sup>12</sup>, is a 2-byte parameter derived from the “integral of the rectified voltage signal over the duration of the AE hit”. Although PAC energy has the same definition as signal strength, the difference is in sensitivity, size and dynamic range of this parameter.

Absolute energy is defined as “the integral of the squared voltage signal divided by the reference resistance (10K-Ohm) over the duration of AE waveform”. This feature is the true energy measure of the AE hit. Unit for absolute energy is atto-joules.

Kaiser Effect is the absence of detectable acoustic emission at a fixed sensitivity level, until previously applied stress levels are exceeded.

Other variables such as peak definition time (PDT), hit definition time (HDT) and hit lockout time (HLT) are classified as system timing parameter.



PDT enables the determination of the time of the true peak of the AE waveform. The main requirement is to avoid false measurements being made on a high-velocity, low amplitude precursor, subject to this, PDT should be as short as possible. A reasonable value to pick PDT is  $L/V$  where  $L$  is the distance between two sensors and  $V$  is the velocity of the fastest wave.

HDT enables the system to determine the end of the hit, close-out the measurement processes and store the measured attributes of the signal. HDT should be at least twice as long as PDT. HDT must be long enough to span over an interval in which the signal to be measured falls below the threshold.

HLT inhibits the measurement of reflections and later arriving parts of the acoustic emission signal so that data from wave arrivals can be acquired at a faster rate. HLT circuitry is a non-triggerable one shot, triggered by the time-out of the HDT. HLT should at least be 300 microseconds for meaningful AE data.

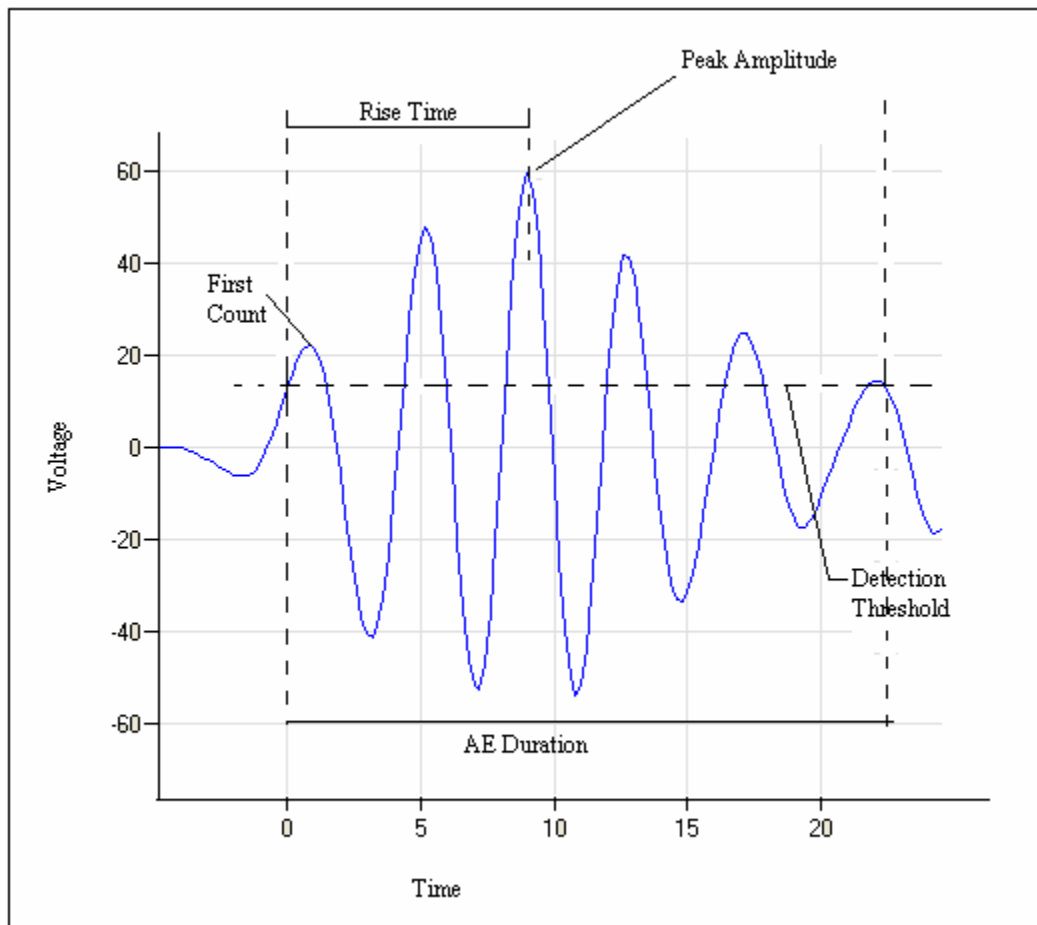


Figure 3.2: Typical Acoustic Emission Signal.

### **3.2 Acoustic Emission Testing**

There are two approaches in which acoustic emission testing is classified. One is Conventional Acoustic Emission testing and other is Quantitative Acoustic Emission testing.

#### **3.2.1 *Conventional Acoustic Emission Monitoring***

In Conventional AE testing, features of acoustic emission signal so called acoustic emission parameters, are measured by analog circuitry. These parameters are plotted against other experimental parameters such as load, strain, or temperature of the test specimen. After repeated tests, experimental implications can be made about the emissions. Typical features or AE parameters used for this purpose are peak amplitude, rise time, duration, energy, and counts above threshold. This approach has been used in number of applications successfully such as structural monitoring, materials testing and process testing.

The conventional AE testing has seen number of successful approaches along with certain disadvantages. One of the major disadvantages is relating the measured AE parameter with the source strongly depends on the geometry and material of the specimen. This is because of the effect that these parameters have on the measured waveform and the AE parameters. Therefore, the application of the technique has been generally limited to situations where large numbers of identical specimens are available for testing, which would help to establish the relationship. Another limitation is its sensitivity with the choice of transducer and detection electronics used for signal acquisition. If the, location of the transducer on the specimen, the bonding of the transducer to the specimen, or the resonant frequency of the transducer are varied, the

detected waveforms and thus the measured AE parameters can be entirely different. Changes in the detection electronics such as the amount of signal amplification or filtering bandwidth also produce changes in the measured parameters. Furthermore, the measured AE patterns are sensitive to variables such as the detection threshold voltage level.

### 3.2.2 *Quantitative Acoustic Emission Testing*

In order to get rid of the changes in the waveforms by the material, transducer, and electronics, research has been carried out in an area commonly referred to as quantitative AE. This research is popular as it characterizes the source function that created the AE wave which was then altered by the effects of propagation and detection. To accomplish this goal, a transfer function is established, whereby it was assumed that the AE waveform was altered by two effects. The first effect was that caused by the geometry of specimen and material, in the propagation of the signal from the source to the detection location. The second effect accounts for the transducer and detection electronics.

### 3.3 Instrumentation

The AE monitoring system used, comprised of PCI-2 “2 Channel AE system on a Card”, AE Win software used to control data acquisition, AE sensors and pre-amplifiers manufactured by Physical Acoustic Corporation.

#### 3.3.1 *System Hardware*

The Physical Acoustics, PCI-2 “2 Channel AE system on a card” is a 2 Channel, AE data acquisition and digital signal processing system. Superior low noise and low threshold performance can be achieved with this AE system. 18 bit A/D conversion and 40 MSPS (mega sample per sec) acquisitions can be achieved with this board without any sacrifice in AE performance. High performance PCI (Peripheral Component Interconnect) bus and separate Direct Memory Access (DMA) architecture for each channel enables significant AE data transfer speed along with waveform transfer capability. The 32 bit PCI bus is standard bus connection in all the computers being used today. Therefore, PCI-2 AE System cards can be installed in most of the computers. The incoming AE signal is passed through an attenuator and buffer circuitry with selectable gain and then passed to the selectable filter circuitry where high pass and low pass filters are applied in accordance with the user programmed filter strategy. The filtered signal is passed through 18 bit, 40 MSPS (mega sample per second) A/D converter where the AE signal is digitized at the, user selectable, rates of up to 40 MSPS. The built-in hit detection and processing circuit performs feature extraction.

Acoustic emission sensors convert the energy carried by the elastic wave into an electrical signal hence, are termed as transducers. Transducers most often used in AE

applications are piezoelectric transducers. Piezoelectric materials are used because of their high sensitivity and ruggedness. To take the advantage of sensitivity, the transducer should be mounted in such a manner that there is minimal loss of acoustic energy at the transducer-material interface. The use of some kind of couplant is necessary for detection of low level acoustic signals. The purpose of the couplant is to ensure good contact between the two surfaces at microscopic level is achieved. Most commonly used couplants are petroleum grease, water, ultrasonic couplants etc. Pre-amplifiers are used to amplify the detected AE signals before they are processed by the system software. The pre-amplifiers used for AE testing are 2/4/6 pre-amplifiers manufactured by Physical Acoustic Corporation, which provide a selectable gain of 20dB, 40dB and 60dB. WD (wide band) sensors from Physical Acoustics were used during the experiments. A single AE sensor and the related equipment components for transmitting, conditioning, detecting and measuring the signals, constitutes an AE channel. Each channel used to monitor AE requires its own sensor, preamplifier and its associated cables.

### 3.3.2 *System Software*

The software which complements, PCI-2 board for data acquisition and signal processing, is AE Win. It is Windows based user friendly software developed by Physical Acoustic Corporation. AE Win handles two different kinds of files, namely initialization and data files.

The initialization files which are distinguished by suffix “.INI” hold all the AE test setup information, i.e. it stores the hardware information, graph information, acquisition and location setup, filter setup, etc. The data files have an extension “.DTA” and are used to store the collected AE data from the structure during the test. This allows

you to re-plot and analyze all the previously collected data files. AE Win has various toolbars such as Setup icon toolbar, acquisition control, line dump, status and statistical toolbar. AE Win has exceptional graphing capabilities. The user can setup multiple 2D or 3D graphs. Many different types of graphs can be set including 2D-line graphs, histograms, scatter point graphs, waveforms, FFT's etc. Graphs can be zoomed or panned for close-up analysis.

The following steps should be taken when carrying out a test:

- Load an appropriate layout file (.LAY) into the system. Make required changes in the hardware setting, channel selection, location layout etc. and save the layout file.
- Enter in acquisition mode. Make sure that the “Save to DTA file (Autodump)” box is checked if you want to save the data.
- Select a name for the data file which needs to be saved.
- Start acquisition mode
- Look at various graphs, data listing, and location plot during acquisition.
- Exit data acquisition.

### 3.3.3 *AE Data Display*

AE data can be viewed in several different ways. The software has the options to create graphs depending upon the user's requirements. AE activities can be measured by counting variable such as number of hits or events. AE signal intensity can be counted by measuring the variables, such as amplitude, energy and counts etc., associated with individual signal.

AE data display can also be classified as:

- History Plots
- Distribution Plots
- Location Plots
- Correlation Plots

History plot shows the chronological course of the test. A typical history plot would be a measure of AE quantities such as counts, energy, events, amplitude, hits or events as a function of load or time. The plot may show cumulative emission, i.e., total activities detected since the start of test, or rate of emission, i.e., AE activity detected within each time increment.

Distribution plot shows the statistical properties of recorded AE data. Typical distribution plots shows number of AE hits and number of waveforms collected versus time. Distribution plots are user selectable. User can add any number of plots required and specify a variable on X-axis and a variable on Y-axis. For example, user can create a graph with number of hits on X-axis and Channel number on Y-axis. Further user can change the graph settings and make it a scatter-point graph, histogram or from other available options depending upon the needs.

Location plot in AE win has two modes, Zonal and Linear location modes. Zonal location is a mode where the first hit sensor of an event group is identified. Zonal location is useful for locating the sensor getting the first hit from a group of sensors. The first hit sensor defines a source zone or area, where that AE event emanated from. Linear location determines a location between two sensors of an event group. Two types of linear location plots are available, one dimensional and two dimensional plots. In one



dimensional plot, the X-axis is a direct mapping of structure. The Y-axis shows AE parameters such as events detected from each X-axis position on the structure, amplitude of events detected from the structure or the duration of these events. Two dimensional plots are more complicated wherein the X and Y-coordinates of the source position are denoted by X and Y-axis respectively.

### 3.4 Lamb Waves

Many structures in practice have plate or shell like characteristics, wherein one of the dimensions is much smaller than the other dimensions. In materials of such geometries, elastic waves propagate in modes, whose propagation characteristics depend upon the plate thickness and frequency of signal along with usual dependence of elastic property and density of the material. These modes are commonly called Lamb waves because of the early studies by Lamb<sup>13</sup> in-to their propagation. There are three types of waves propagating, one is out-of-plane plate deformations which are symmetric about mid-plane and are referred as symmetric mode, second is out-of-plane plate deformations which are anti-symmetric about mid-plane and are referred as anti-symmetric mode and third mode has transverse particle vibrations which are horizontal to the surface of plate and are referred as shear horizontal or SH modes. Figure 3.3 shows phase velocity dispersion curve while Figure 3.4 shows group velocity dispersion curve for plate like structure, which are developed with the help of software called “PAC dispersion curve” prepared by Physical Acoustic Corporation.<sup>14</sup>

Acoustic emission signals propagate as extensional (symmetric) and flexural (anti-symmetric) plate modes in thin plate like geometries such as shells, pipes, and tubes. The relative amplitude of two modes depends on the directionality of source motion. For out-of-plane motions, such as delaminations or particle impact, the flexural or bending plate mode dominates the signal with only a small extensional mode detected. A signal from such a source can be simulated with a pencil lead break (Hsu-Nielsen source) or by an impact on the surface of the plate. For in-plane source motions, such as

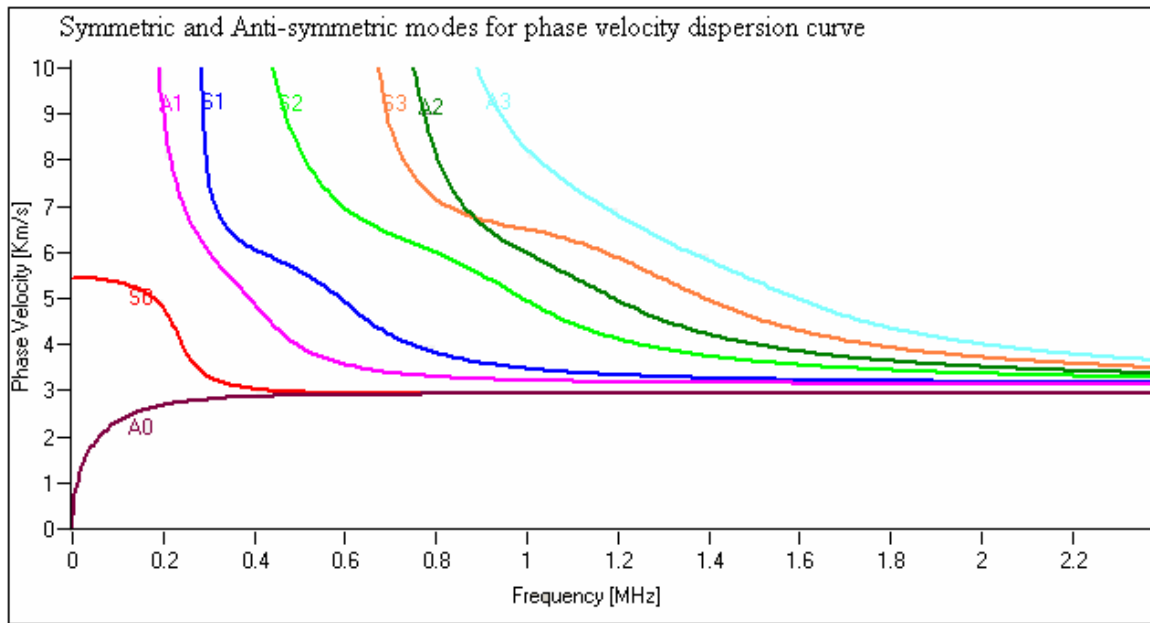


Figure 3.3: Phase velocity dispersion curves for aluminum plate.

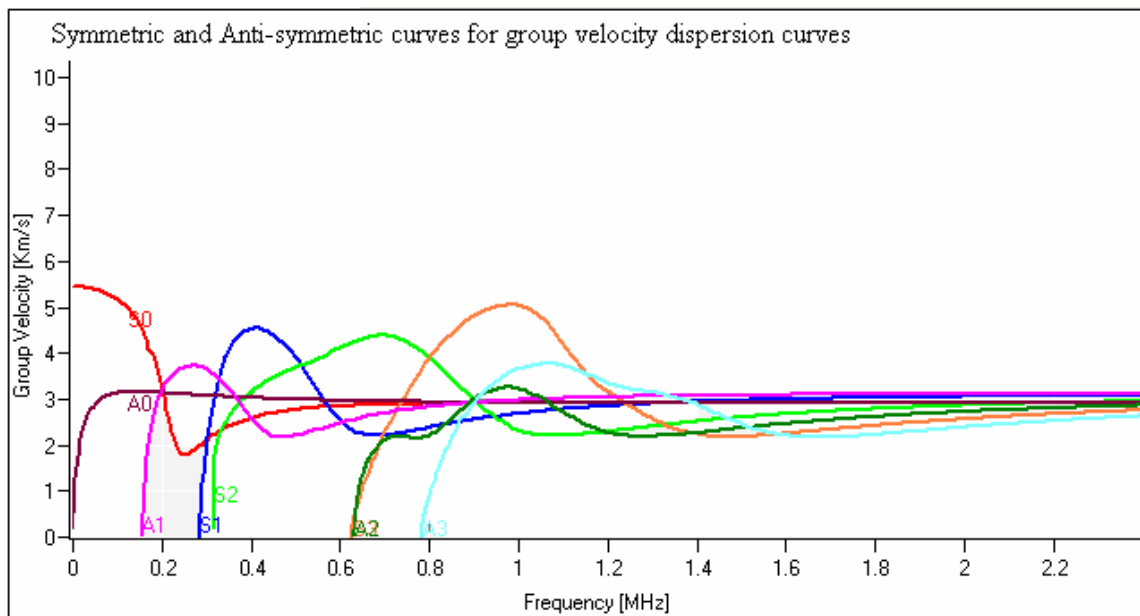


Figure 3.4: Group velocity dispersion curve for aluminum plate.

matrix cracking or fiber breakage, the extensional mode dominates the signal with very small flexural modes. Signals from these types of sources can also be simulated with a pencil lead break or impact, however the impact or lead must be fractured at the edge of the plate rather than on its surface to produce in plane source motion.

Impact force on the surface of plate produces out-of-plane motion and the signal acquired contains both flexural as well as extensional mode. It was found out by Prosser<sup>15</sup> that during low velocity impacts the signals are dominated by large flexural modes with very less extensional modes present. Extensional mode signals are high frequency signals and travel with high velocity therefore appearing before flexural modes in the acquired signal. For high velocity impact the acoustic emission signals contain dominant extensional and flexural modes. The relative amplitude of both the modes is high compared to low velocity impact. There are two significant differences observed while analyzing the signals from low velocity impact and high velocity impact. First, the signals contain much higher frequencies and second, large extensional mode component are present in the signal. Figure 3.5 shows the typical signal produced due to low impact and Figure 3.6 shows the signal produced due to high impact on the plate.

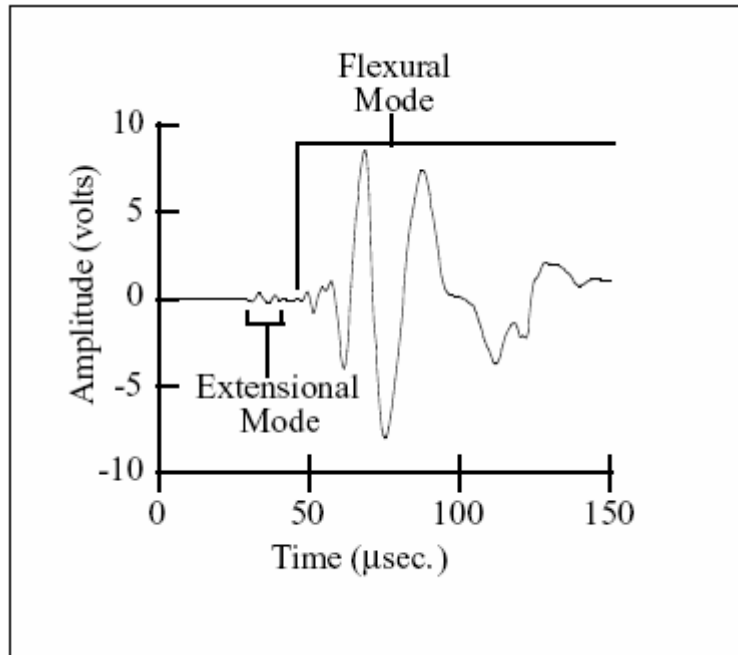


Figure 3.5: AE Signals produced due to low velocity impact on plate.

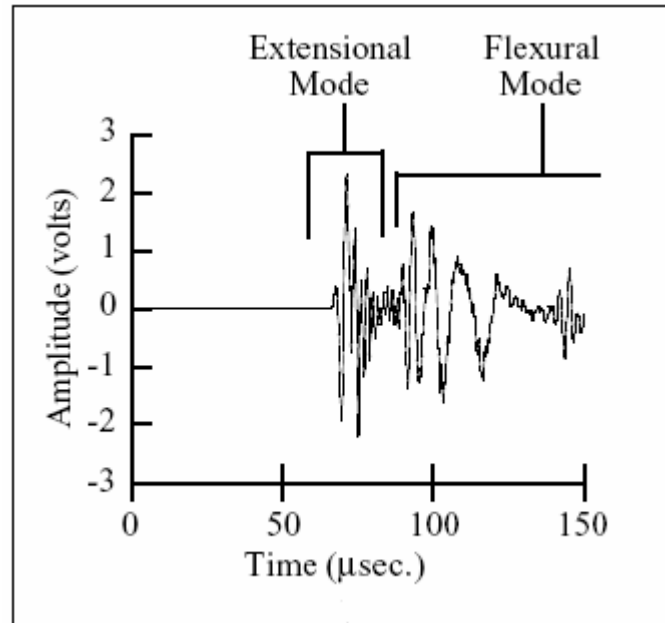


Figure 3.6: AE Signals produced due to high velocity impact on plate.

## **CHAPTER FOUR: METHODOLOGY**

The instrumentation involved for the tests includes acoustic emission data acquisition board (PCI-2 card), AE sensors and pre-amplifiers, from Physical Acoustic Corporation. The experiments are performed with two thin metal strips of different materials, aluminum and steel. A calibration test is always performed prior to AE monitoring to ensure that the signals acquired by hardware board and instrumentation involved are not distorted. To maintain a good contact at microscopic level between the sensor and material, “Vaseline” is used as a couplant. Calibration test also helps to find out whether there is any damage to the instrumentation or the software being used is functioning well. Procedure for calibration test and its results are explained below.

### **4.1 AE Calibration Test**

Calibration test for acoustic emission monitoring is conducted under controlled test conditions. The calibration test procedure remains the same irrespective of the material type. A sample calibration test is described next where thin aluminum strip was used as test specimen.

The aluminum strip used, was 2.44 m in length, 0.025 m wide with thickness of 0.0032 m. Two acoustic emission broadband sensors were used to detect the location of source. Simulated acoustic emission signals were generated by performing pencil lead break (Hsu-Nielsen source) on the surface of the specimen used. Linear source location technique was used for test, to determine the location of the pencil lead break. When the linear location of the pencil lead breaking is analogous with the measured one, it confirms that the instrumentation is working up to expectation.

For the test, location of sensors is specified with respect to defined coordinate system for the strip. Location of sensor, connected to Channel-1 is assumed at (0, 0) and location of sensor, connected to Channel-2 is at (1.5, 0). The position of source is calculated from the difference in arrival times between hits for both the channels. Input value of wave velocity for the specimen is calculated by conducting an initial test. A pencil lead break test is performed between the two sensors, such that it is 0.254 m away from channel-1 and 1.27 m away from channel-2. The schematic representation is shown in Figure 4.1. The extra distance traveled by the signal traveling towards channel-2 is divided by the difference in arrival time of signal for both the channels to get wave velocity. In this particular case, the extra distance traveled by the signal towards channel-2 is 1.02 m, which is divided by the difference in arrival time (222  $\mu$ s), to give the wave velocity of 16475 km/h. The hardware settings for the acquisition board are controlled by the software AE Win. The pre-amplifier gain is selected as 40dB, frequency bandwidth is kept at 20 KHz – 1 MHz, sampling rate is 5 MSPS (mega sample per second), pre-trigger was set as 50 and 1024 points were collected. The calculated value of wave velocity is substituted in the software for calculating exact linear location of the source during further trials. This gives the confirmation that the AE sensors and the instrumentation provide the desired output. A test was conducted to find out the location of pencil lead break performed at the center, and on the surface of the plate. Linear location of the event occurred between the two sensors is shown in Figure 4.2. Figure 4.3 shows a signal produced due to pencil lead break on the surface of the aluminum strip.

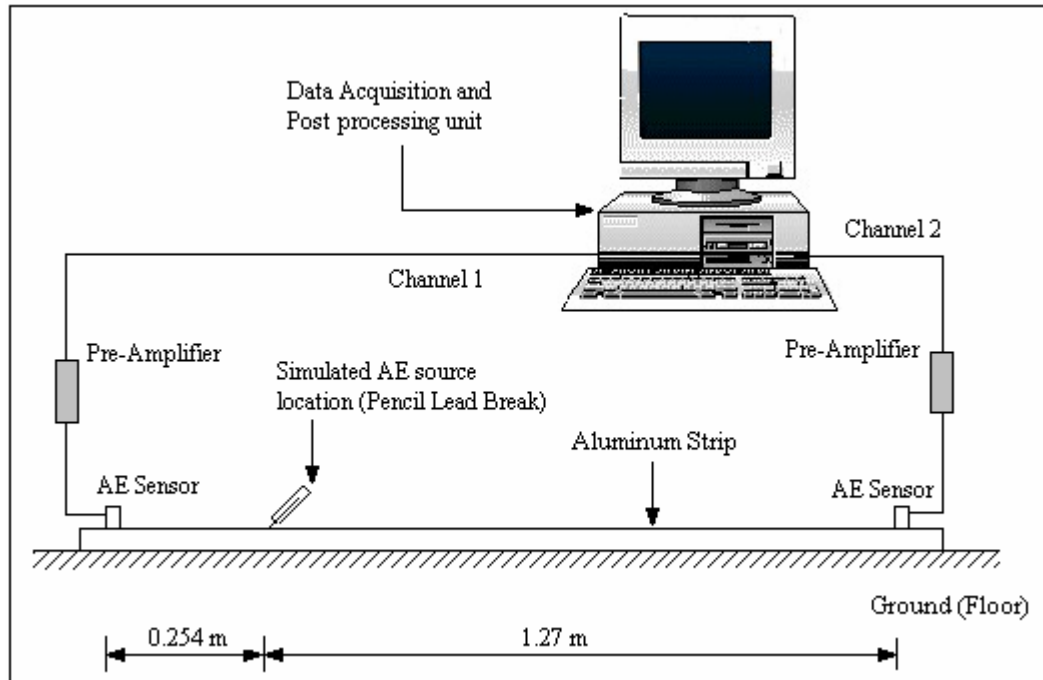


Figure 4.1: Schematic representation of pencil lead break test to calculate velocity.



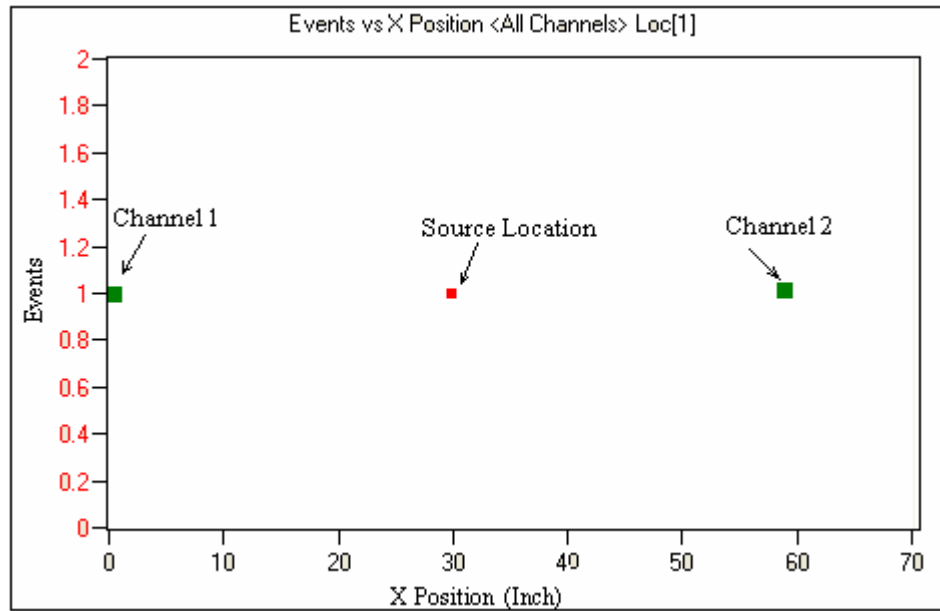


Figure 4.2: Plot of Events Vs Position for Test.

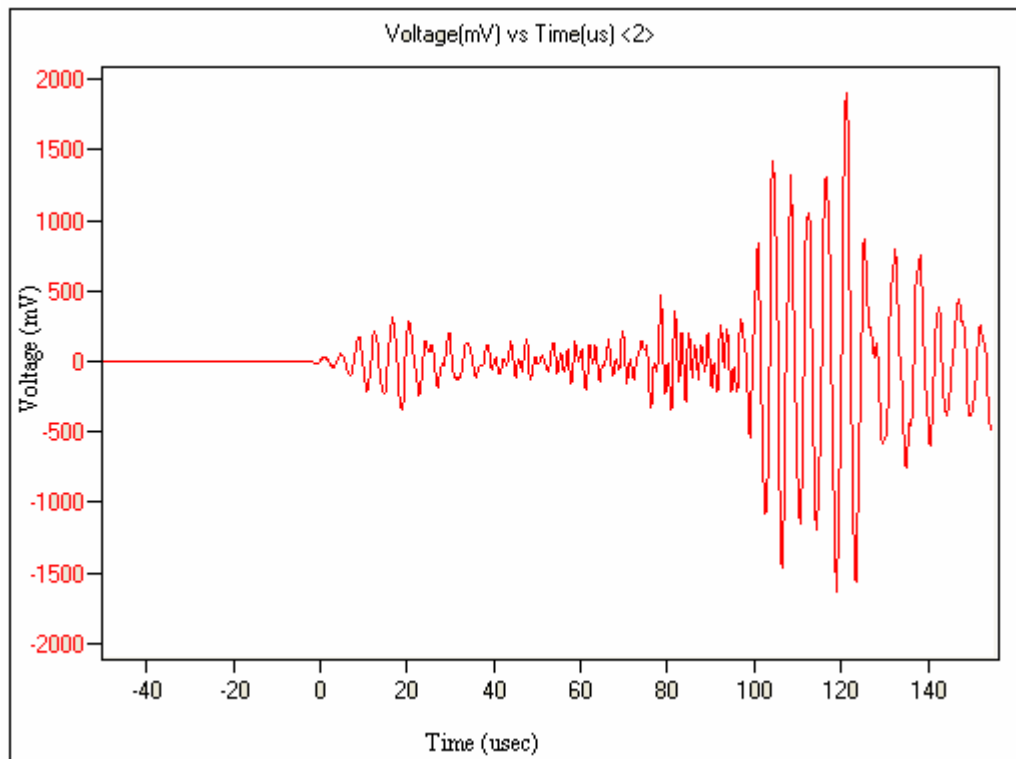


Figure 4.3: A typical signal produced by pencil lead break on the surface of strip.

## 4.2 Frequency Bandwidth Selection

As discussed earlier an impact on thin plates produces acoustic emission signals which propagate as symmetric and anti-symmetric modes with different frequencies. The velocity of the waves traveling depends on frequency of the signal. The frequency content of any signal depends upon the type of the impact. As the impact varies from low impact to high impact the extensional modes become dominant. It is very important that both sensors get triggered by the same mode to get exact location and orientation of the source. In this particular case, where we are using aluminum strip and since the sensors are placed at large distance, precaution should be taken while selecting the frequency bandwidth. The higher frequency signals attenuate faster and do not travel long distance. So if the sensors are too far away from the point of impact it might happen that the sensors gets triggered by different modes resulting in incorrect location calculation. Also if sensors get triggered with two different modes, the detected waveforms, and thus the measured AE parameters, will be entirely different. The best way to find out frequency bandwidth is from the dispersion curve for that particular material and thickness of the specimen. From the dispersion curve we can find the velocity of first anti-symmetric or flexural mode and use it to trigger the sensors instead of first symmetric or extensional mode. Also we need to narrow the frequency filter so that the higher frequency extensional mode gets filtered out. From dispersion curves the frequency bandwidth for aluminum strip, of thickness 3.175 mm, is found to be 20 kHz – 400 kHz with wave velocity of 7132 km/h for the first anti-symmetric mode. However, frequency bandwidth selection for any strip is empirical and also depends on material characteristics.

### **4.3 Material Selection for the Strip**

As we intend to use a thin strip for the WIM system, we need to select the strip material suitably. The dynamic force applied by the tires on strip will be high. The strip could undergo plastic deformation under such high impact forces. Hence, we need to design the strip in order to avoid its plastic deformation because the acoustic emission activities reduce significantly once the plate undergoes plastic deformation. Also, the strip must be attached firmly to ground because any relative motion or friction between the strip and ground may generate unnecessary acoustic signals which are basically noise. Under these conditions it is very difficult to determine the signal produced due to impact. The other major cause of concern is Kaiser Effect in elastic materials due to application of impact force, which is discussed further in the next section. Also there are signals generated due to relative motion of tire with the surface of plate, especially when the vehicle is running slowly which might be reduced by increasing the threshold value.

### **4.4 Kaiser Effect due to Impact Force**

Kaiser effect is defined as the absence of detectable acoustic emission until previously applied stress levels are exceeded. We need to find out what generates the acoustic emission signals when tire passes over the strip. It might be friction between the strip and ground, it might be the friction between the tire and strip or it might be structural signals as material yields. However, the signals generated by friction between ground and strip, are taken care of by attaching the strip firmly to ground. It is very difficult to control the signals generated due to friction between wheel surface and strip. It is evident that as the vehicle moves fast, the contact time between the tire and strip is reduced and hence fewer acoustic signals are generated due to the friction. These signals

might be filtered using a high threshold value. We are interested in the signals which are generated mainly due to impact force exerted by the tires on strip. We need to monitor Kaiser effect during the application of impact force. If there are structural signals generated during the impact then Kaiser effect would be significant as the strip is repeatedly loaded and unloaded. To avoid this we need to select the strip material of high strength and which does not yields or deforms under impact force.

Test was carried out on both aluminum and steel strips for impact loading. The dimensions of aluminum strip are 2.44 m long, 0.0254 m wide and 0.0032 m thick, while dimensions for steel strip were 1.128 m long, 0.03175 m wide and 0.0032 m thick. The strip is taped to ground to restrict its motion in all direction. Two acoustic emission broadband sensors were used during the test. Linear location technique is used for source location, i.e. location of the impact. Figure 4.4 shows the schematic representation of the test, showing the position of sensors and location of impact force.

In the test discussed aluminum strip was used as specimen. For the test, sensor location was entered in such a way that the sensor for channel-1 is placed at (0, 0) and the sensor for channel-2 is placed at (1.524, 0). Impact force was generated with the help of a steel ball drop from a specific height on the specimen. An initial calibration test was conducted to find the velocity of wave traveling towards the sensors corresponding to impact. Wave velocity is calculated by the same procedure described before. Once the wave velocity is calculated it is entered in software for calculation of exact location of impact, which ensures that the signals acquired by sensors are not distorted.

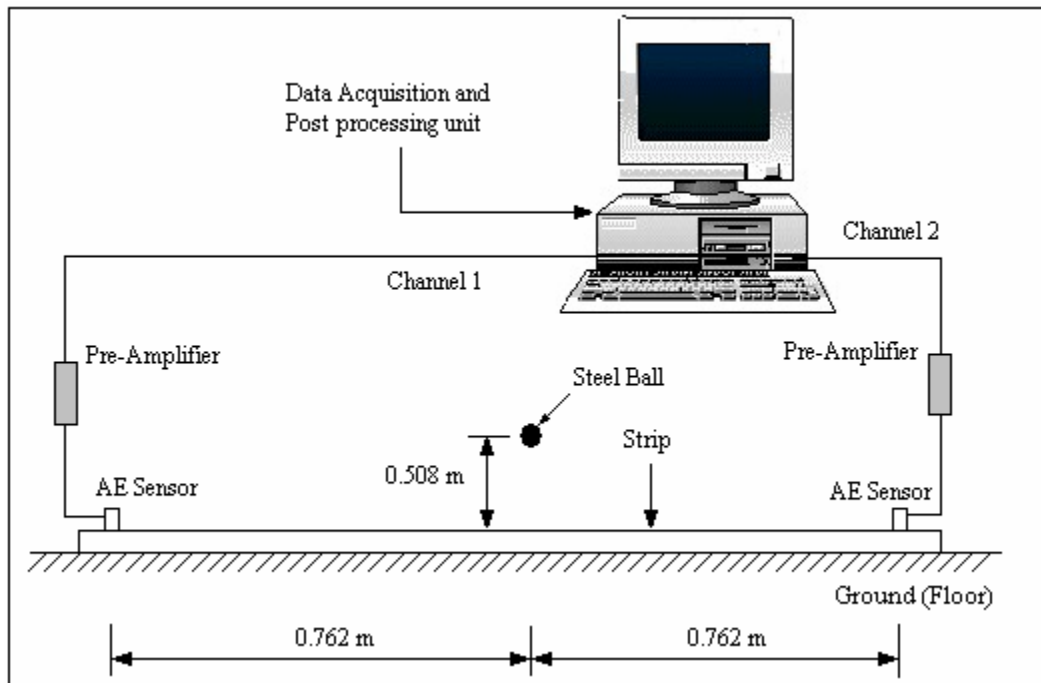


Figure 4.4: Schematic representation of the test for monitoring Kaiser Effect.

A constant impact force was applied for 10 trials at the same location. The ball which weighs 3.18 gm (0.00318 kg) was dropped from a height of 0.508 m, producing impact energy of 0.019 J. Acoustic emission parameters such as counts, energy, amplitude, and absolute energy were monitored. For an impact test if the signals are structural signal or if the applied impact force is causing significant damage to the strip then AE parameters would decrease for successive trials showing the presence of Kaiser effect. Figure 4.5 shows a typical AE signal generated due to impact force produced with the help of steel ball on aluminum strip.

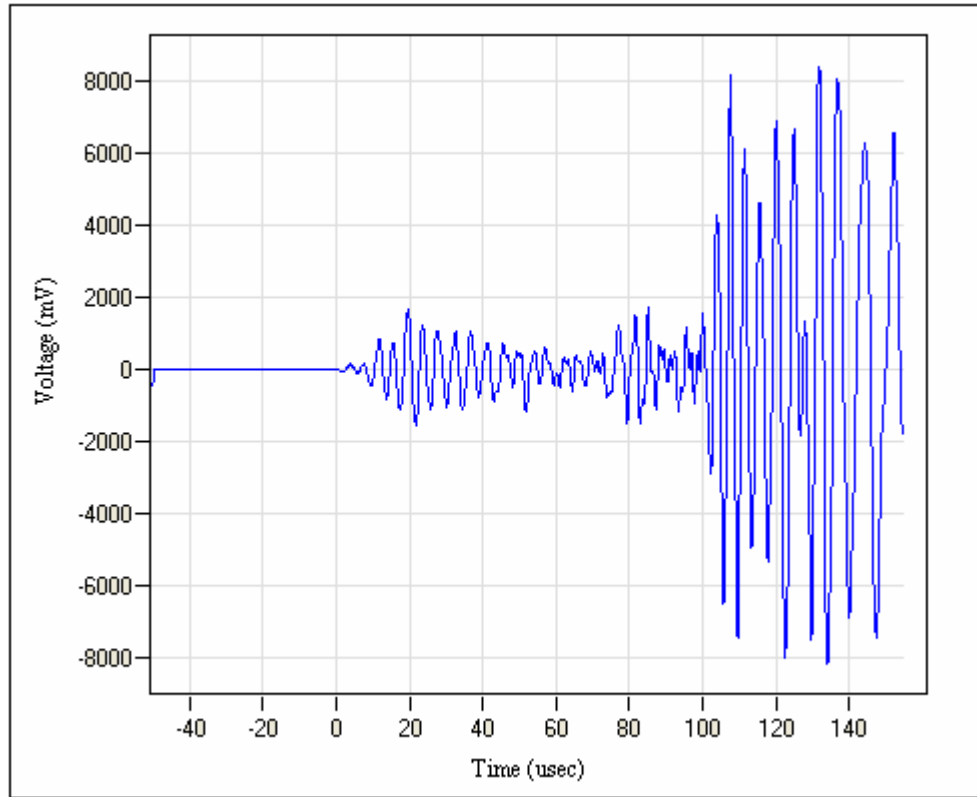


Figure 4.5: A signal generated due to impact force on aluminum strip.

Table 4.1 shows the acoustic emission parameters acquired by channel-1 where as Table 4.2 show the acoustic emission parameters acquired by channel-2 during the test. Figure 4.6 shows the variation of acoustic emission counts w.r.t. number of trials for signals acquired through channel-1 while Figure 4.7 shows the variation of acoustic emission counts w.r.t. number of trials for the signals acquired through channel-2. It was found that the number of counts do not show a decreasing trend for successive trials. Further Figure 4.8 and Figure 4.9 shows the variation of signal energy w.r.t. number of trials for the signals acquired through channel-1 and channel-2 respectively. It is found that signal energy doesn't show any decreasing trend with successive trials using same

impact force. Hence, AE activities do not tend to decrease with repeatedly loading and unloading resembling no Kaiser effect.

Table 4.1: AE parameters acquired by channel-1 when constant impact force is applied for 10 trials.

Trials	Counts	Energy (mV- $\mu$ sec)	Duration ( $\mu$ sec)	Amplitude (dB)	Absolute Energy(aJ)
1	904	10076	14208	94	130.33
2	949	12926	14348	94	166.15
3	795	10321	11188	94	132.91
4	793	13435	11890	94	178.32
5	924	11324	14286	94	150.05
6	805	13020	13470	94	169.96
7	1083	10837	13975	94	142.39
8	867	9390	12356	94	118.06
9	847	13130	11882	94	170.76
10	706	11702	9395	94	154.82

Table 4.2: AE parameters acquired by channel-2 when constant impact force is applied for 10 trials.

Trials	Counts	Energy (mV- $\mu$ sec)	Duration ( $\mu$ sec)	Amplitude (dB)	Absolute Energy(aJ)
1	1404	12532	14487	94	157.04
2	1065	16017	14110	94	207.39
3	1085	13114	13355	94	180.88
4	1018	16284	14094	94	214.39
5	1471	13655	14461	94	174.53
6	1146	15361	13957	94	204.21
7	1430	13672	14381	94	176.82
8	1493	12192	14736	94	158.68
9	945	15732	13844	94	204.02
10	787	14083	13370	94	191.34

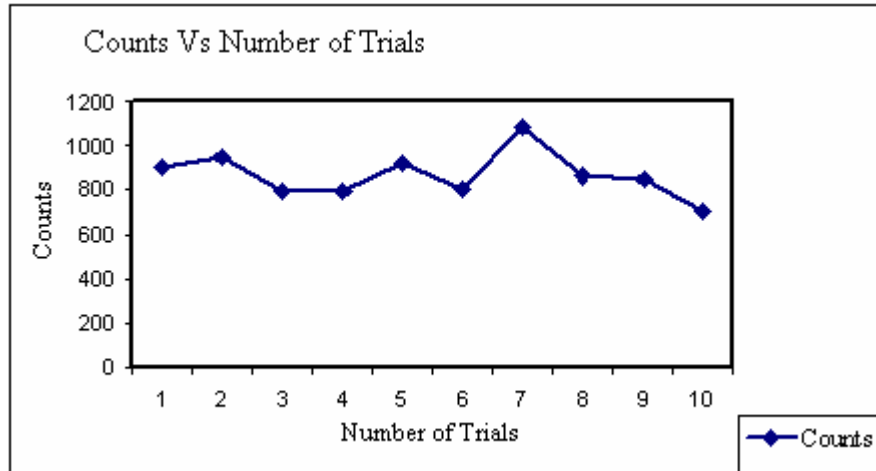


Figure 4.6: Variation of AE Counts for 10 trials collected by Channel-1.

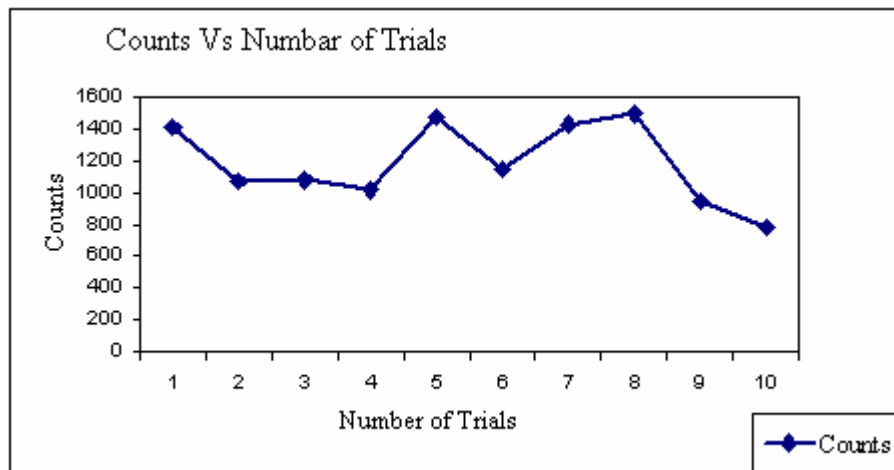


Figure 4.7: Variation of AE Counts for 10 trials collected by Channel-2.



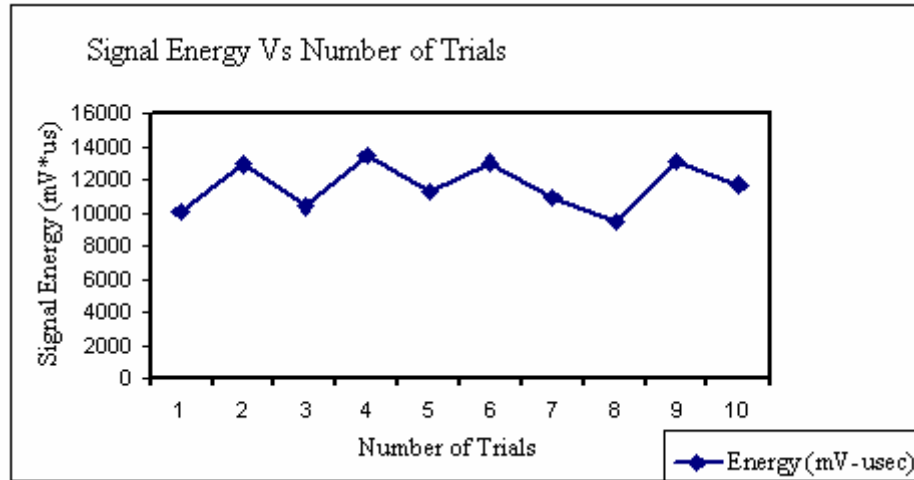


Figure 4.8: Variation of Signal Energy for 10 Trials collected by Channel-1.

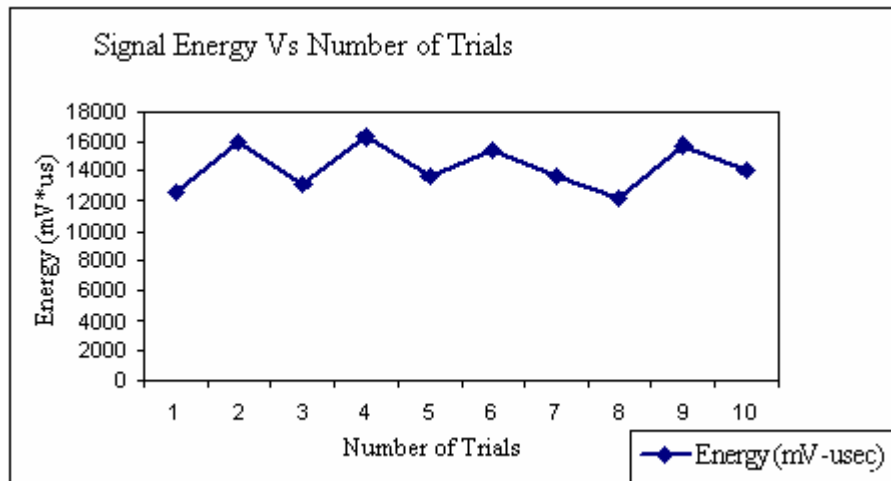


Figure 4.9: Variation of Signal Energy for 10 Trials collected by Channel-2.

#### **4.5 Variable Impact Force**

We are monitoring the acoustic emission signals which are generated due to impact force exerted by tire on to the strip. Hence it becomes necessary to study whether there is any correlation between acoustic emission parameters with that of varying impact force. The test is conducted on both aluminum and steel strips.

For the test discussed herein Aluminum strip is used as a test specimen. A variable impact force is generated by dropping a steel ball from different height level on to the specimen. The weight of the ball is 3.18 gm (0.00318 Kg). Precaution must be taken such that the acoustic signals are generated purely due to impact and it does not damage or deform the strip. The strip was taped to the ground firmly and two acoustic emission sensors were attached at end of the strips. The ball was dropped at the center of strip that is 0.762 m from both the sensors. Linear source location technique was used to find the location of impact. The frequency bandwidth is selected as 20 kHz- 400 kHz according to the procedure described earlier. A threshold of 45dB, pre-amplifier gain of 40dB, a sampling rate of 5 MSPS (mega sample per second) is used and 1024 points are acquired. The linear location technique confirms that both the sensors are triggered by same frequency signal and the acquired signals are not distorted. The schematic representation of the test is shown in Figure 4.10. The ball is dropped from different heights. The height is increased in a step of 0.254 m until 1.778 m. The acoustic emission parameters recorded includes counts, amplitude, signal strength and absolute energy.

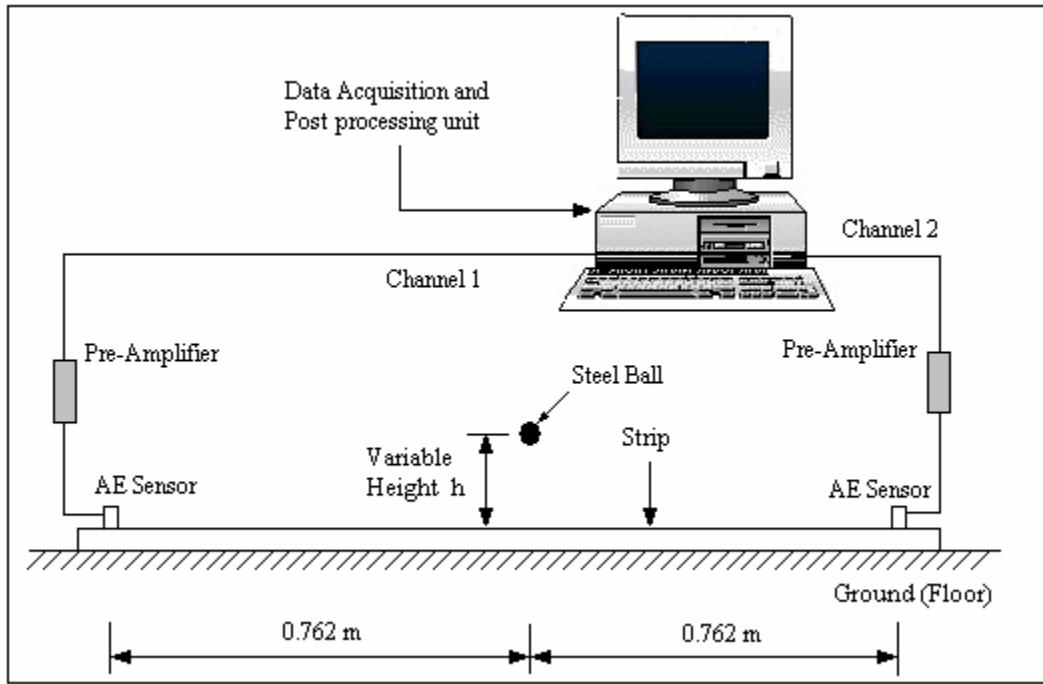


Figure 4.10: Schematic representation of Variable impact test on aluminum strip.

Figure 4.11 shows the variation of counts w.r.t. impact energy for the signals acquired from channel-1, while Figure 4.12 shows the variation of counts w.r.t. impact energy for the signals acquired from channel-2. It is found that, the number of counts goes on increasing with the increase in impact force. A linear regression was found between the counts and impact energy, with a regression coefficient of about 0.92. Figure 4.13 shows the variation of signal energy w.r.t. impact force for the signals acquired through channel-1, while Figure 4.14 shows the variation of signal energy w.r.t. impact force for signals acquired through channel-2. The graph shows that the energy of the signal increases with increase in impact energy. A linear regression was found between signal energy and impact energy with a regression coefficient of about 0.97. Figure 4.15 shows the variation of absolute energy of the signals acquired through channel-1 w.r.t.

the impact energy while Figure 4.16 shows the variation of absolute energy w.r.t. impact energy for signals acquired through channel-2. A linear regression was found between absolute energy of the signals and impact energy with regression coefficient of 0.95. It is found that linear regression is the best fit between the acoustic emission parameters and the variable impact force.

Table 4.3: AE parameters acquired by channel-1 when variable impact force was applied.

Trials	Height (Inches)	Impact Energy (J)	Measured AE Parameters			
			Counts	Energy (mV-usec)	Amplitude (dB)	Absolute Energy (aJ)
1	10.000	0.010	785	10415	94	136070
2	20.000	0.019	803	11132	94	142087
3	30.000	0.029	983	14439	94	202756
4	40.000	0.038	1007	15312	94	189654
5	50.000	0.048	1200	18283	94	237316
6	60.000	0.057	1598	21272	94	276096
7	70.000	0.067	1668	22788	94	297405

Table 4.4: AE parameters acquired by channel-2 when variable impact force was applied.

Trials	Height (Inches)	Impact Energy (J)	Measured AE Parameters			
			Counts	Energy (mV-usec)	Amplitude (dB)	Absolute Energy (aJ)
1	10.000	0.010	1015	11076	94	141802
2	20.000	0.019	1062	13296	94	180422
3	30.000	0.029	1142	15914	94	214393
4	40.000	0.038	1313	16267	94	216875
5	50.000	0.048	1728	19807	94	256405
6	60.000	0.057	1998	24559	94	325986
7	70.000	0.067	2104	27056	94	363840

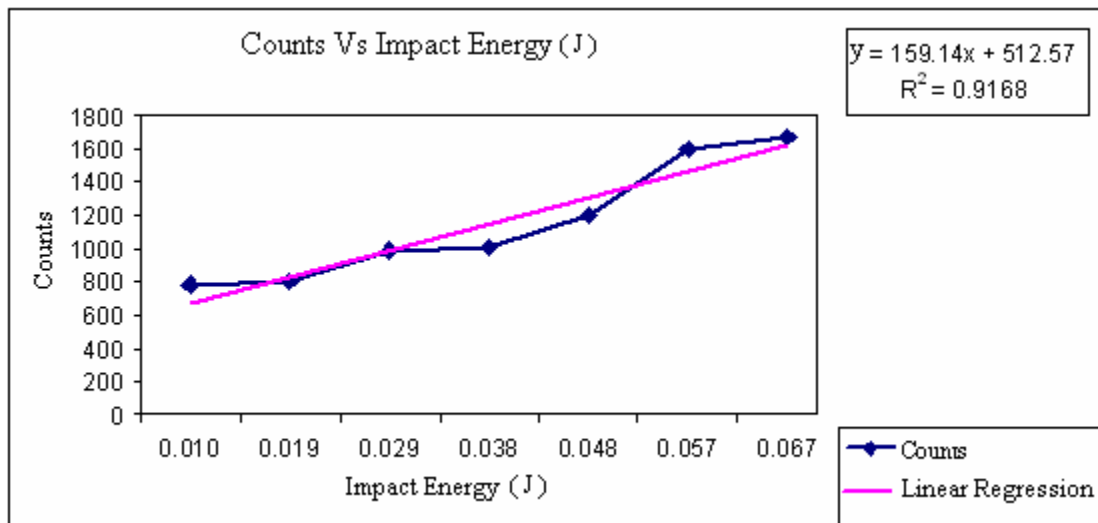


Figure 4.11: Variation of counts w.r.t. impact energy for signals acquired through channel-1.

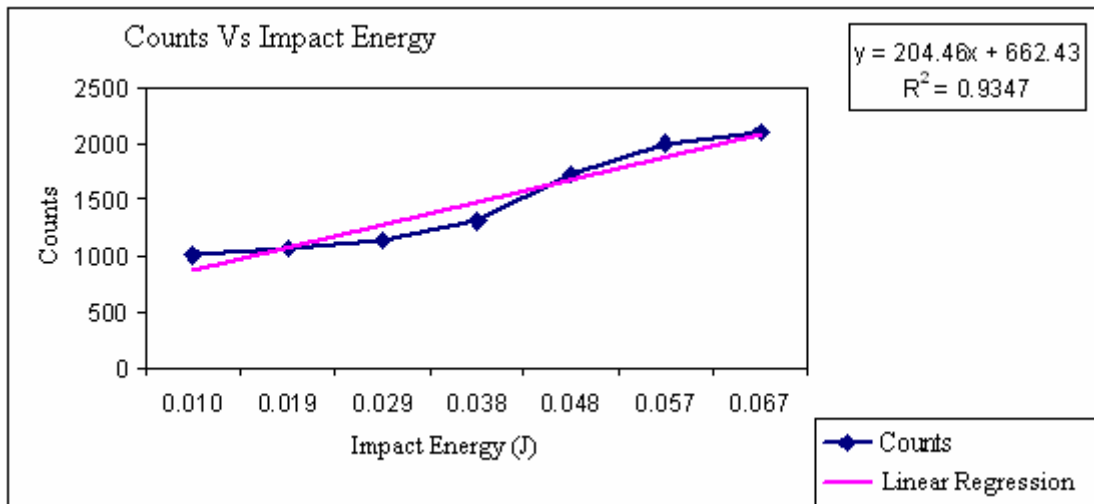


Figure 4.12: Variation of counts w.r.t. impact energy for signals acquired through channel-2.

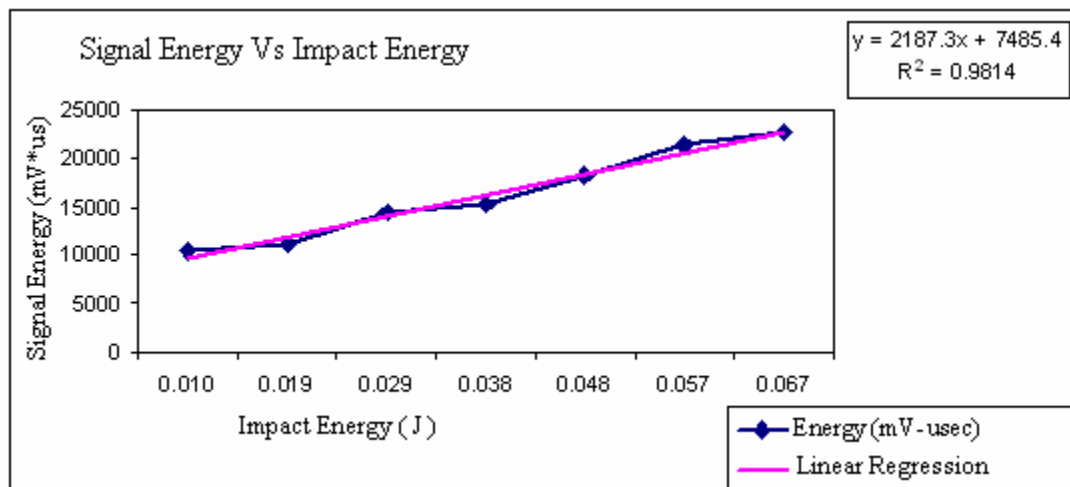


Figure 4.13: Variation of signal energy w.r.t. impact energy for signals acquired through channel-1.

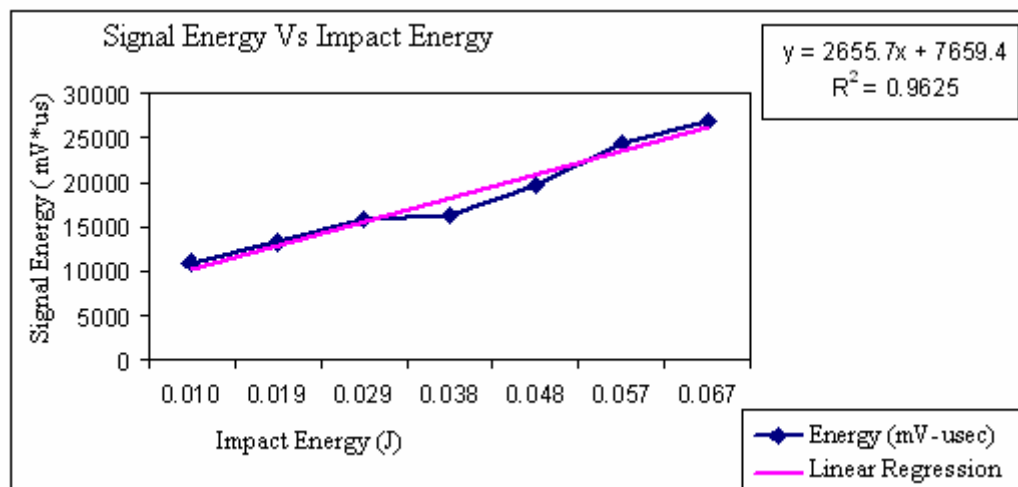


Figure 4.14: Variation of signal energy w.r.t. impact energy for signals acquired through channel-2.

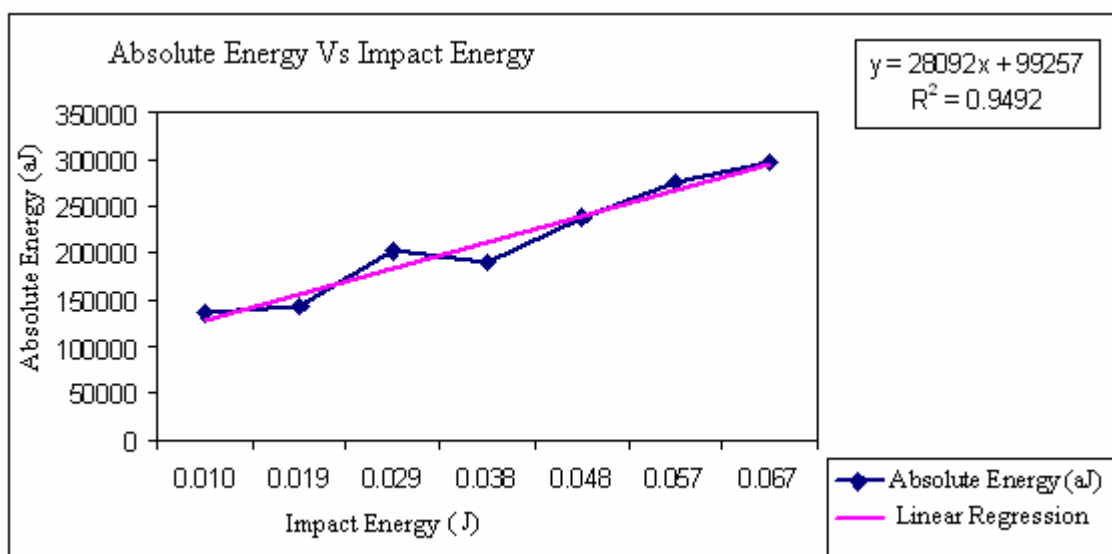


Figure 4.15: Variation of absolute energy w.r.t. impact energy for signals acquired through channel-1.

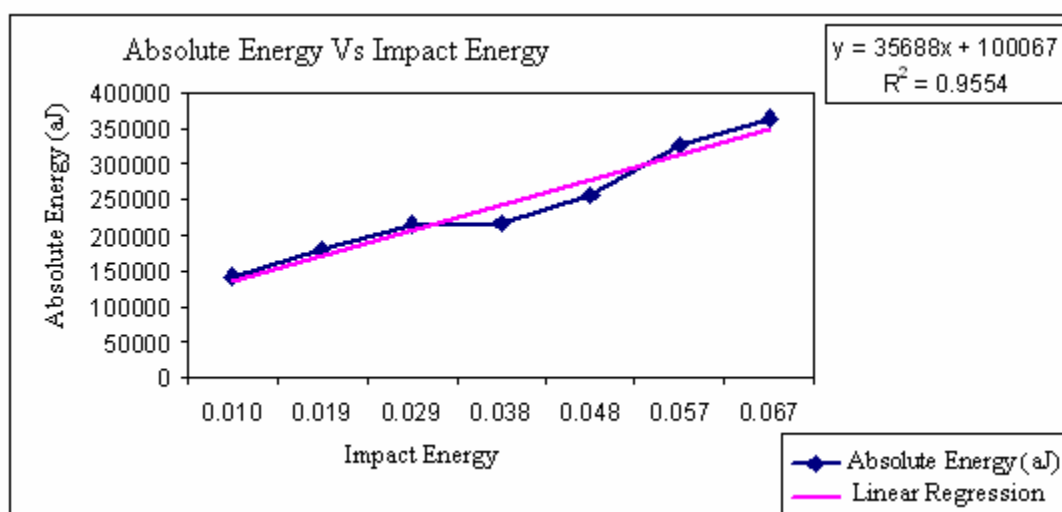


Figure 4.16: Variation of absolute energy w.r.t. impact energy for signals acquired through channel-2.

## CHAPTER FIVE: TESTING AND RESULTS

Till now we have conducted the initial calibration of the system along with initial experimentation to monitor Kaiser effect due to impact loading. Also variation of acoustic emission parameters with variable impact load is studied. Now the experiments were performed along the same principle, by riding a bike and driving a car over a metal strip. The goal is to correlate the impact produced, during wheel passage over strip, with the acoustic emission parameters.

### 5.1 Bike Test

A bike test was carried out by riding the bike over the strip with different velocities. The concept was to develop a correlation between the speed of bike and acoustic emission parameters and the test was conducted under controlled test conditions. The aluminum strip was tapped to ground firmly to avoid any relative motion of the strip with the ground. A double sided tape was used between the strip and the ground in order to avoid noisy signals generated due to friction between the strip and ground. A calibration test was conducted to check the system. The frequency bandwidth was selected as 20 kHz – 400 kHz along with sampling frequency of 2 MSPS, pre-amplifier gain of 40 dB, and 1024 points were acquired. The schematic representation of the test is shown in Figure 5.1. The location from where the bike crosses over the strip was kept at the center of strip i.e 0.762 m away from both the sensors.

Table 5.1 shows the acoustic emission parameters acquired during the test. It is found out that the passage of bike over the strip does not produce much impact and most of the signals are produced due to friction between wheel and strip surface.



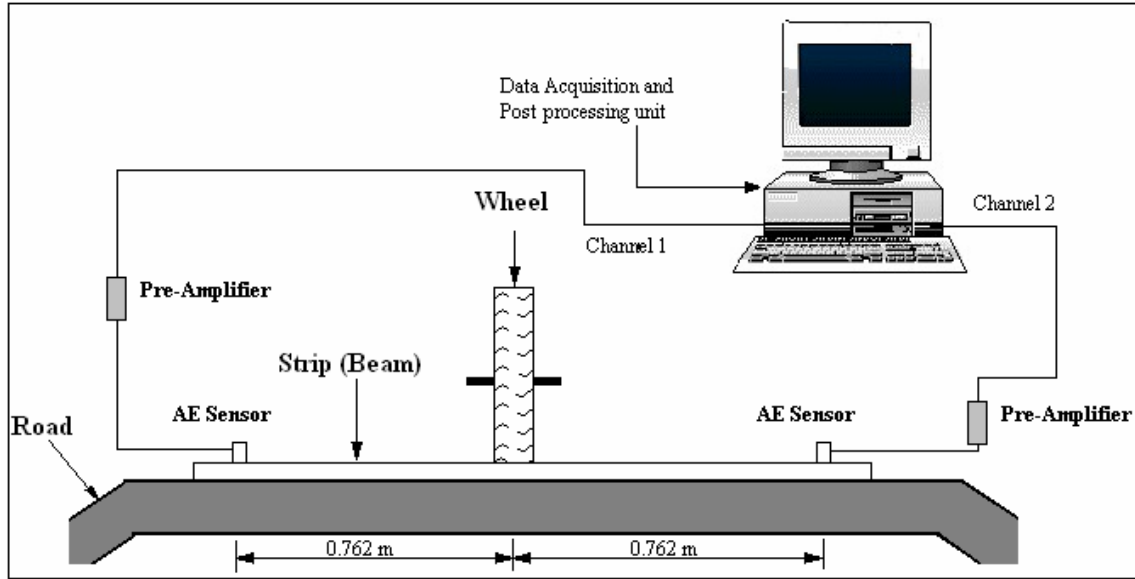


Figure 5.1: Schematic Representation of Bike test.

Table 5.1 Acoustic emission parameters acquired during bike test.

Trials	Measured AE Parameters			
	Counts	Energy (mV*us)	Amplitude (dB)	Absolute Energy (aJ)
1	40	4	46	287.799
2	40	1	49	237.148
3	30	3	58	84.074
4	7	0	41	16.592
5	58	6	38	433.447
6	46	5	49	296.716
7	22	2	48	77.274
8	37	4	44	16.114

## 5.2 Car Road Test

Two different types of tests were carried out. For the first test, the velocity of the car was varied and an attempt to develop a correlation, between the velocity of the car and acoustic emission parameters was made. In the second test the velocity of the car was kept constant while the weight was varied so that it generates different impact force every time it crosses the strip.

### 5.2.1 *Car Test with Varying Speed*

The test is carried out in such a way that for each trial the velocity of car was varied. The make and model of the car used for testing was 2002 Honda Civic. The gross vehicle weight of the car is 1250 kg. The test was carried out on both the aluminum and steel strips. The strips were firmly taped to the ground next to each other and single sensor is used on each of the strip. Figure 5.2 shows the photo taken during the experiment and the sensors attached to it. Figure 5.3 shows the test setup. A double sided tape was used between the strip and ground interface to avoid direct contact of the strip with the ground. A single sensor was attached to the end of the strip. The schematic representation of the test is shown in Figure 5.4. A calibration test was carried out in order to check the instrumentation. The frequency bandwidth was set to 20 kHz – 400 kHz. The sampling rate was set to 2 MSPS (mega sample per second), pre-trigger was set to 50, and threshold of 50 dB was used in order to filter the noisy signals produced due to the friction between the tire and the surface of the strip. Less noisy signals are encountered when the car passes with high speed over the strip, representing less contact time between

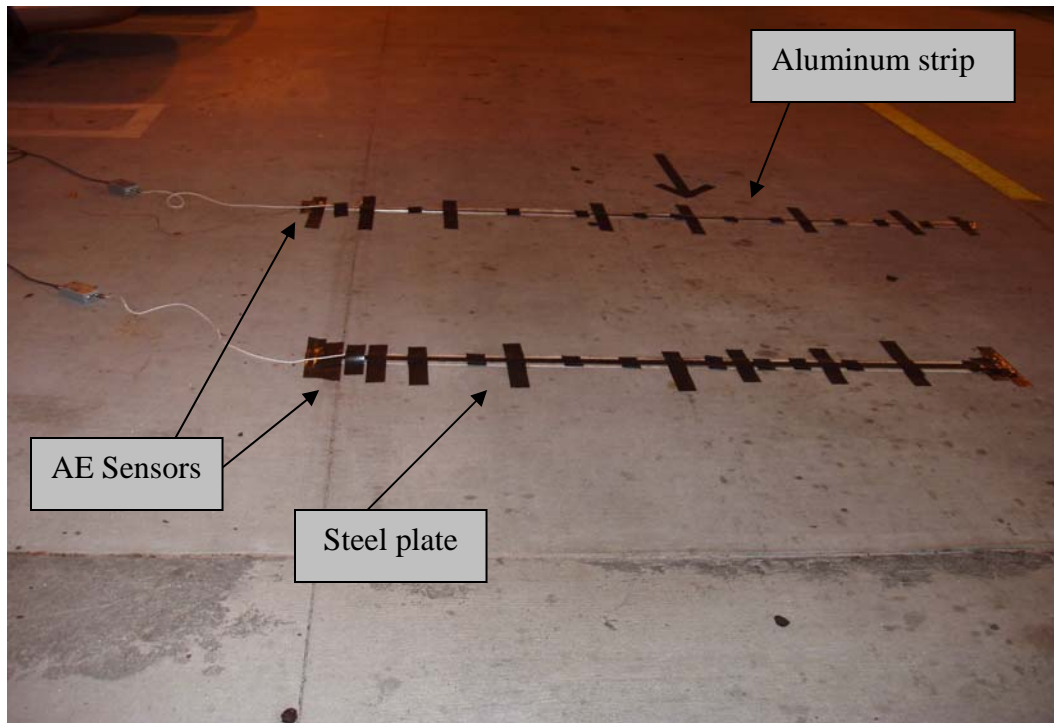


Figure 5.2: Aluminum and Steel strip attached to ground.



Figure 5.3: Test setup during the car test.

the strip and the tire. The speed of the car was varied for each run and acoustic emission parameters were studied. The difference in the arrival time of the signal produced due to the impact from the front wheel and rear wheel is observed out. The velocity of car was found out by dividing the distance between the front axle and rear axle by the difference in the arrival time of the signals. The axle distance for the vehicle used during the test was 107 Inches. Large numbers of signals were generated during each test and we need to differentiate the signals which were produced due to impact, from the signals which are produced through other sources such as friction between wheel surface and strip surface. Also the location of wheel passing over the strip was tried to keep as consistent as possible. Only one of the channels was used for data acquisition in order to avoid damage to the wiring equipment of channel-2 when the vehicle passes over it. Figure 5.5 shows the photograph taken during the car test.

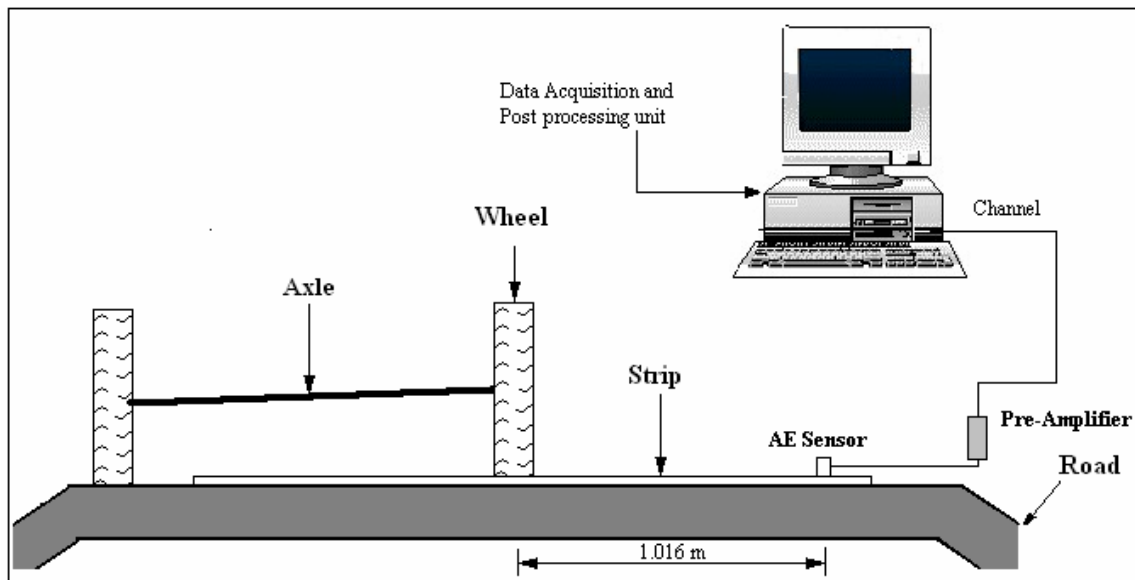


Figure 5.4: Schematic Representation of Car Test.



Figure 5.5: Car test being conducted

The variation of acoustic emission parameters acquired with the variation of speed is listed in Table 5.2, when the front wheel passes over the strip, and Table 5.3, when the rear wheel crosses over the strip. Figure 5.6 illustrates the variation of counts w.r.t. the speed of the vehicle when the front wheel passes over the strip and Figure 5.7 when the rear wheel passes over the strip.

For this case a polynomial correlation of second order was found between the counts and speed of the vehicle with a regression coefficient of 0.95.

The variation of signal energy with the speed of the vehicle is illustrated by Figures 5.8 and 5.9, when the front and rear wheel passes over the strip respectively. Figure 5.10 shows the variation of absolute energy with the speed of the vehicle when the front wheel passes over the strip and Figure 5.11 shows a similar plot when the rear wheel passes over the strip.

In all the abovementioned cases a second order polynomial correlation exists between the acoustic emission parameters and speed of the vehicle. As can be seen from Figures 5.8 to 5.11, the best fit of 0.94 is achieved for signal energy and a best fit of 0.97 is achieved for absolute energy.

Table 5.2: AE results when front wheel passes over the strip.

Trials	Distance Between Axle (Inches)	Time Difference (sec)	Calculated Speed (Km/h)	Measured AE Parameters			
				Counts	Energy (mV.usec)	Amplitude (dB)	Absolute Energy (aJ)
1	107	1.11	9	805	2834	90	8684000
2	107	0.81	12	660	1925	81	3090000
3	107	0.67	15	115	277	69	180576
4	107	0.42	24	334	1258	88	4082000
5	107	0.36	27	1136	4097	89	10933000
6	107	0.32	31	1400	4904	94	32144000

Table 5.3: AE results when rear wheel passes over the strip.

Trials	Distance Between Axle (Inches)	Time Difference (sec)	Calculated Speed (Km/h)	Measured AE Parameters			
				Counts	Energy (mV.usec)	Amplitude (dB)	Absolute Energy (aJ)
1	107	1.11	9	577	1764	88	5246000
2	107	0.81	12	433	909	80	1091000
3	107	0.67	15	134	297	75	144073
4	107	0.42	24	355	1034	92	3594000
5	107	0.36	27	1010	3005	91	10373000
6	107	0.32	31	1493	4081	94	16344000

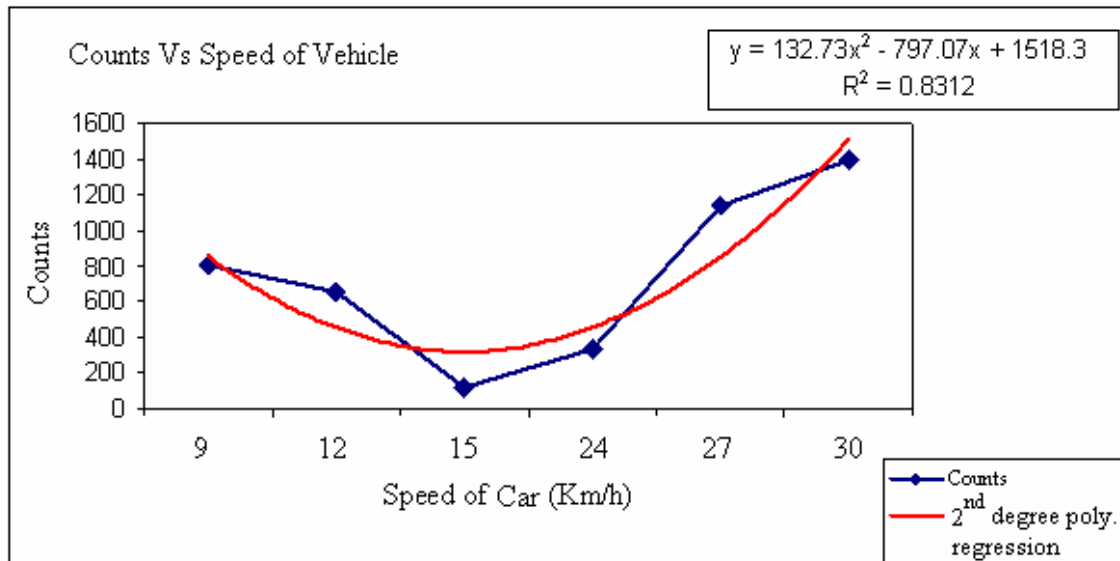


Figure 5.6: Variation of AE Counts w.r.t Speed of vehicle when front wheel passes over the strip.

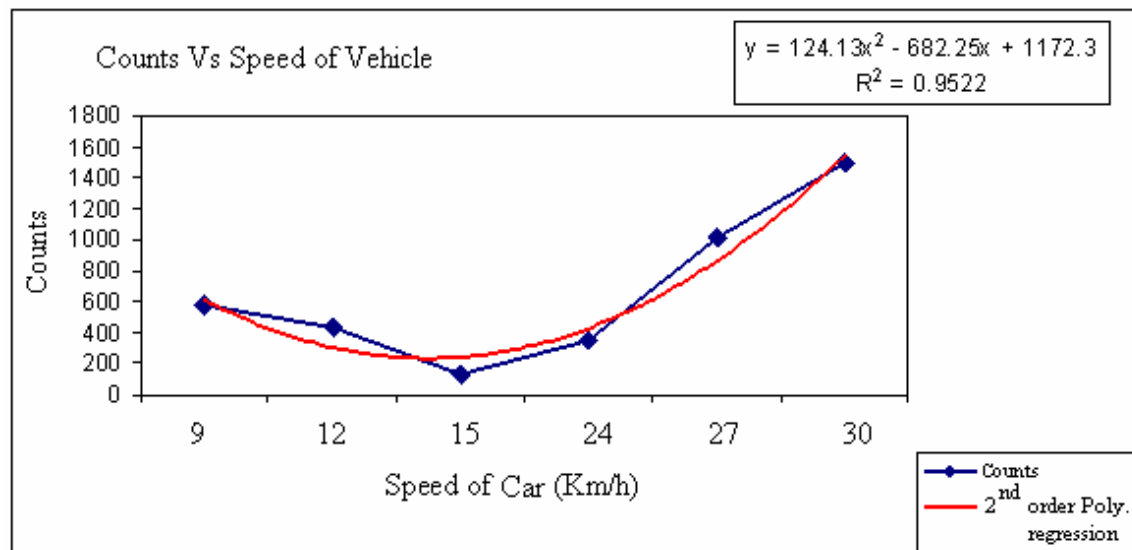


Figure 5.7: Variation of AE Counts w.r.t Speed of vehicle when rear wheel passes over the strip.



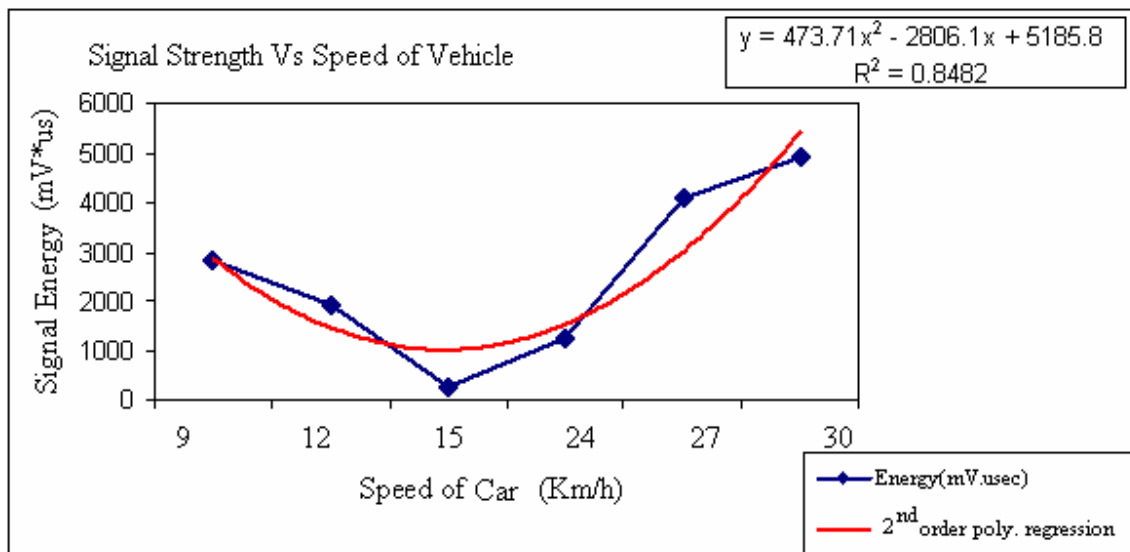


Figure 5.8: Variation of Signal Energy w.r.t. Speed of vehicle when front wheel passes over the strip.

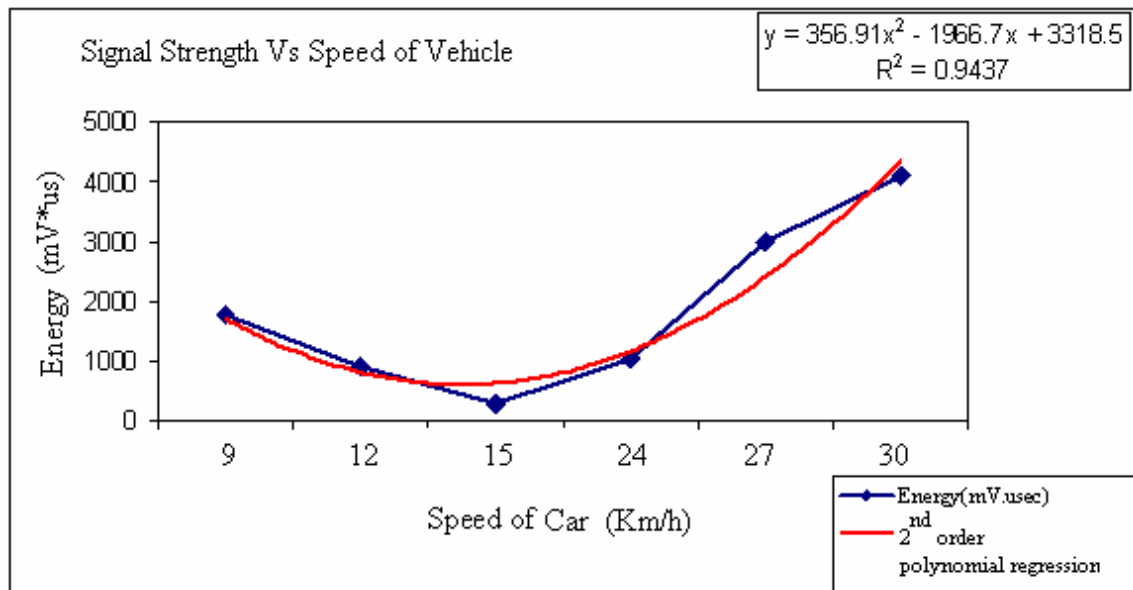


Figure 5.9: Variation of Signal Energy w.r.t. Speed of Vehicle when rear wheel passes over the strip.

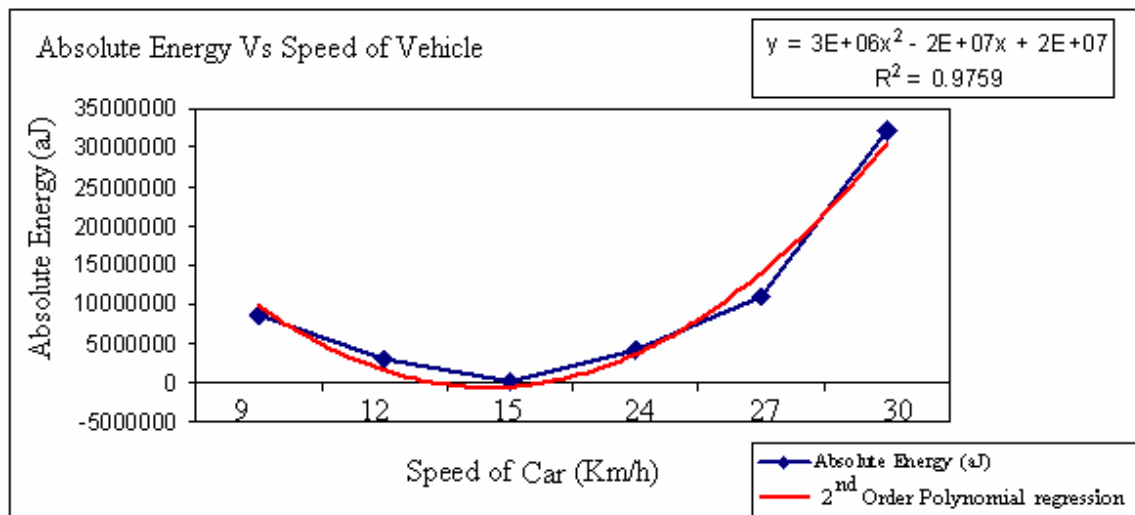


Figure 5.10: Variation of Absolute Energy w.r.t. Speed of Vehicle when front wheel passes over the strip.

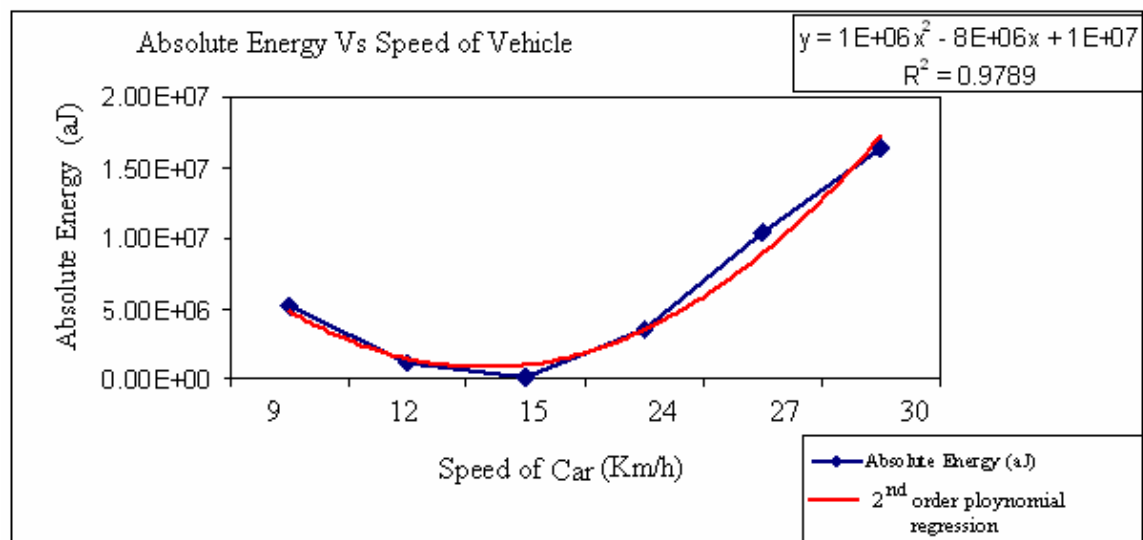


Figure 5.11: Variation of Absolute Energy w.r.t Speed of Vehicle when rear wheel passes over the strip.

### 5.2.2 *Car Test with Varying Weight*

The test was carried out, such that the car passes over the strip with a constant velocity while the weight inside it was varied in successive trials. The make and model of the car used was 2002 Honda Civic having a weight of 1250 kg. The weight was increased in successive trials with increasing the number of passengers within the car. The strip was taped to the ground and a double sided tape was placed between the plate and ground interference to avoid the generation of noisy signals due to friction. The frequency bandwidth was kept at 20 kHz – 400 kHz, sampling rate was set at 2 MSPS, threshold was set at 50 dB, pre-amplifier gain was set at 40 dB, and 1024 points were acquired. Only one channel was used for data acquisition after the calibration was done.

The aforementioned experimental setup, described in section 5.2.1, was used to study the correlation between the acoustic emission parameters and the weight in the car.

An increasing trend in acoustic emission parameters is observed when the weight inside the vehicle is increased. Figures 5.12 and 5.13 illustrates the variation of counts w.r.t. variation of weight in the car for the signals acquired when the front and rear wheel, respectively, passes over the strip.

Figure 5.14 and Figure 5.15 shows the variation of signal energy w.r.t. weight for the signals acquired when the front and rear wheel, respectively, passes over the strip. The acoustic emission parameters acquired when the front wheel passes over the strip is shown in Table 5.3 while Table 5.4 shows similar parameters acquired when the rear wheel passes over the strip. The variation of absolute energy of the signal with the variation of weight is illustrated in Figure 5.16, when the front wheel passes over the

strip, and Figure 5.17, when the rear wheel crosses over the strip. In all the cases a linear relation between the acoustic emission parameters and the weight in the car is observed.

Table 5.4: Acoustic emission parameters acquired when front wheel passes over the strip.

Trials	Counts	Energy (mV* $\mu$ sec)	Duration ( $\mu$ sec)	Amplitude (dB)	Absolute Energy (aJ)
1	81	69	1219	67	26270
2	91	97	2696	65	28250
3	137	136	1207	76	67799
4	151	140	1410	73	89023
5	169	149	3102	68	176200

Table 5.5: Acoustic emission parameters acquired when rear wheel passes over the strip.

Trials	Counts	Energy (mV*us)	Duration ( $\mu$ sec)	Amplitude (dB)	Absolute Energy (aJ)
1	11	14	1140	57	1670
2	29	20	1103	65	4021
3	76	57	1382	77	19751
4	88	63	1668	65	31441
5	103	76	2635	63	36877

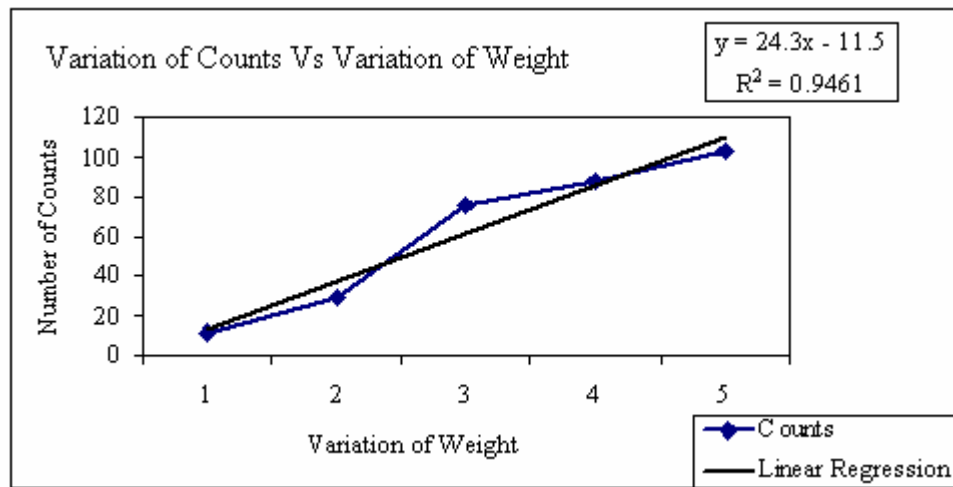


Figure 5.12: Variation of counts w.r.t weight in vehicle when front wheel passes over the strip.

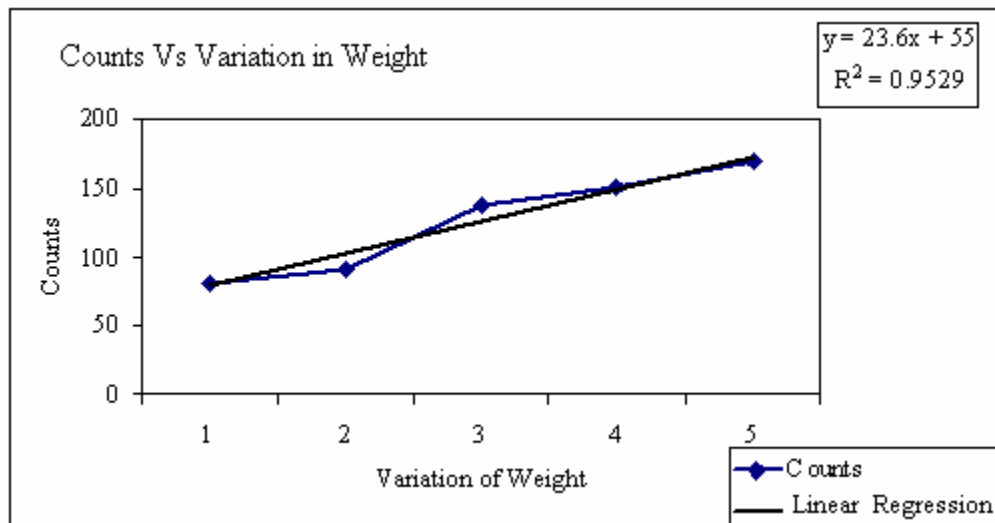


Figure 5.13: Variation of counts w.r.t. weight in vehicle when rear wheel passes over the strip.

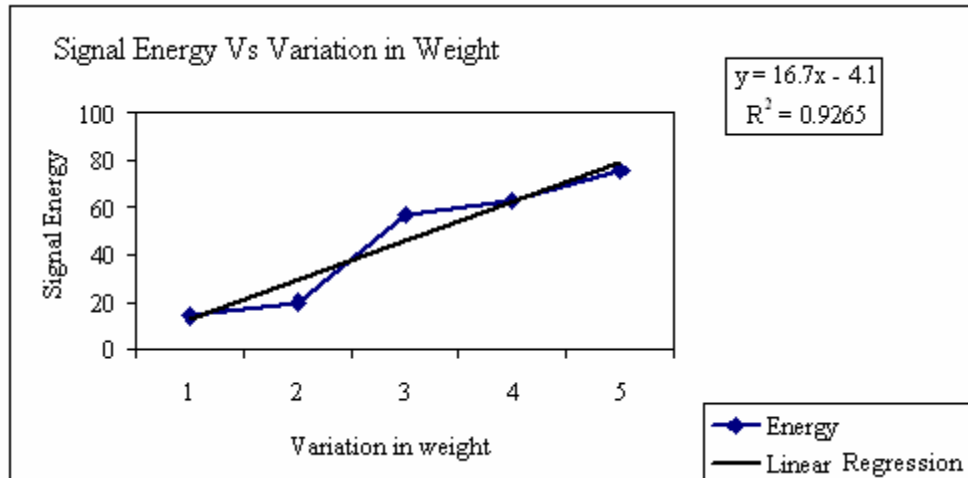


Figure 5.14: Variation of signal energy w.r.t weight in vehicle when front wheel passes over the strip.

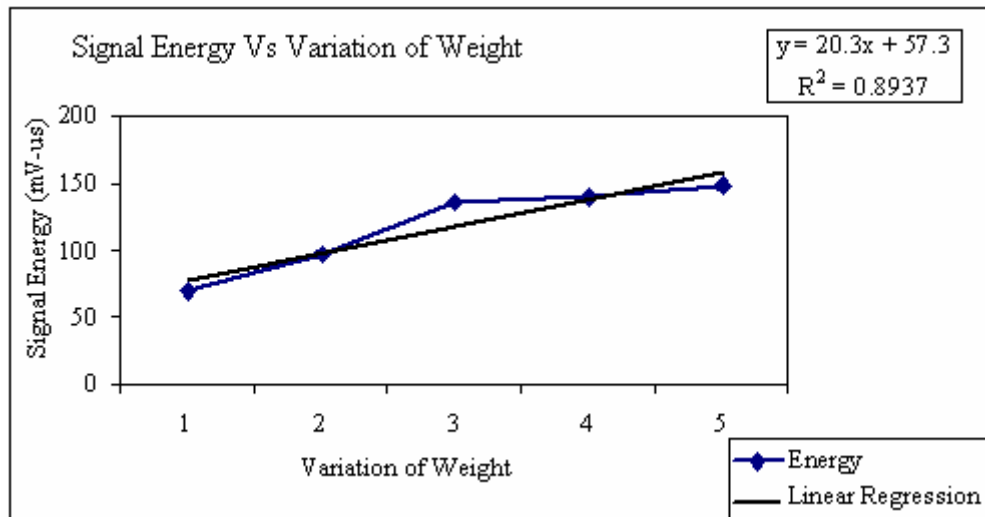


Figure 5.15: Variation of signal energy w.r.t weight in vehicle when rear wheel passes over the strip.

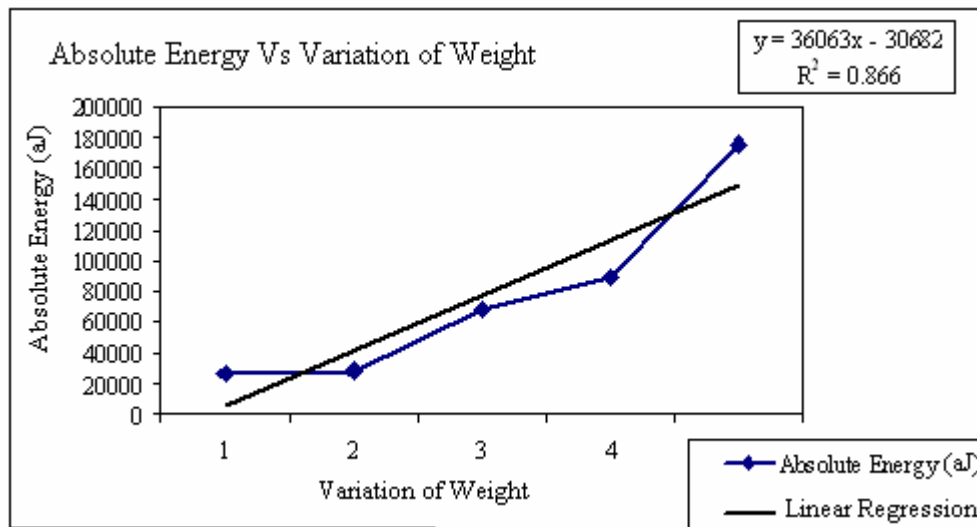


Figure 5.16: Variation of absolute energy w.r.t. weight in vehicle when front wheel passes over the strip.

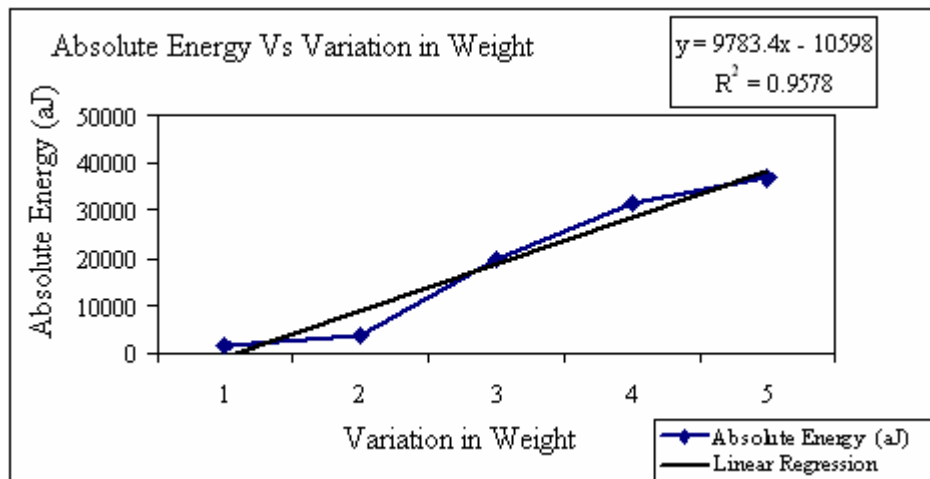


Figure 5.17: Variation of absolute energy w.r.t. weight in vehicle when rear wheel passes over the strip.

From the results, absolute energy gives a better correlation for both the tests conducted and should be used for correlating with weight and speed of car. However other acoustic emission parameters can be explored.

A typical truck tire shows as approximate rectangular contact area with the ground and normally termed as “Footprint”.<sup>16</sup> Total weight of vehicle axle is supported by its tires and is shared by the number of tires. Under-inflation causes a longer footprint of the tire which means larger area of contact with ground and less average pressure. Longer footprint might give rise to more noisy signals due to friction between the tire and strip, also the acoustic emission parameters might reduce because of low average pressure.

The width of the strip should be selected properly as for larger width the time of contact between the strip and tire is more, producing noisy signals due to friction. Also to avoid deformation of the strip, high strength material should be used for strip. The strip should be firmly attached to the ground to avoid any kind of damage caused due to fast moving vehicles.



We conclude this chapter by summarizing some preliminary results, which should be fully investigated in future work. Future work can be done by processing the acquired signals. First, Wavelet transform was used and the maximum wavelet coefficient was correlated with the vehicle weight and speed. An example is shown below by performing wavelet transform on the acquired signals during the variable impact force test. The code to perform wavelet transform was written in matlab which has the following capabilities

1. Reading the data acquired by data acquisition card.
2. Computing the frequency response of the signal acquired.
3. Plotting the time domain plots and frequency domain plots (both linear and logarithmic)
4. Perform wavelet transform of the captured impulse in time domain.
5. Plotting the wavelet coefficient plot over scale and time domain.
6. Get the values of maximum wavelet coefficient.

Figure 5.18 shows the data acquired through the data acquisition card. Figures 5.19 and 5.20, shows frequency domain plots in linear and logarithmic scale respectively while Figures 5.21 and 5.22 shows the plot of 2D wavelet coefficients and 3D wavelet coefficients respectively. The variation in Wavelet coefficient w.r.t. the impact energy is shown in Figure 5.23. It is observed that there is a linear relation between the wavelet coefficients and impact energy.

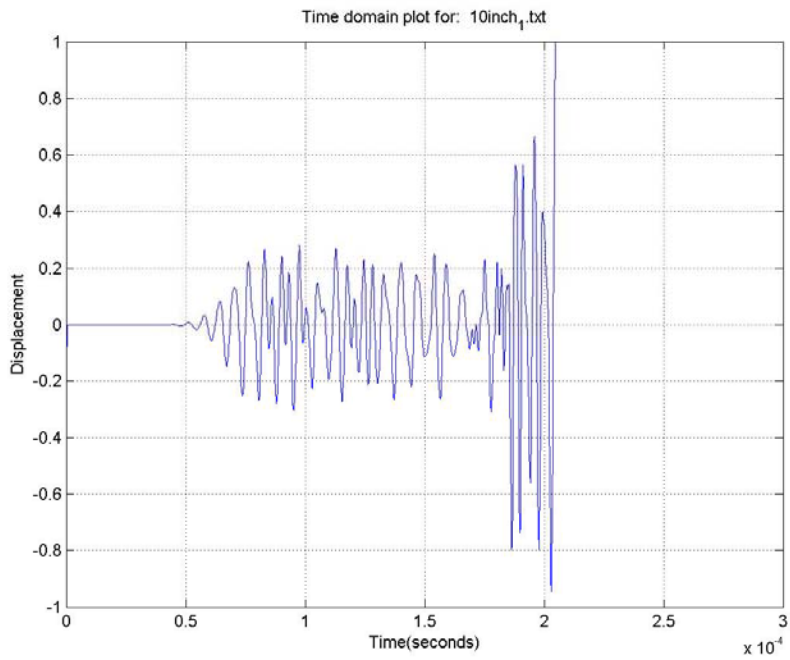


Figure 5.18: Signal acquired by data acquisition card.

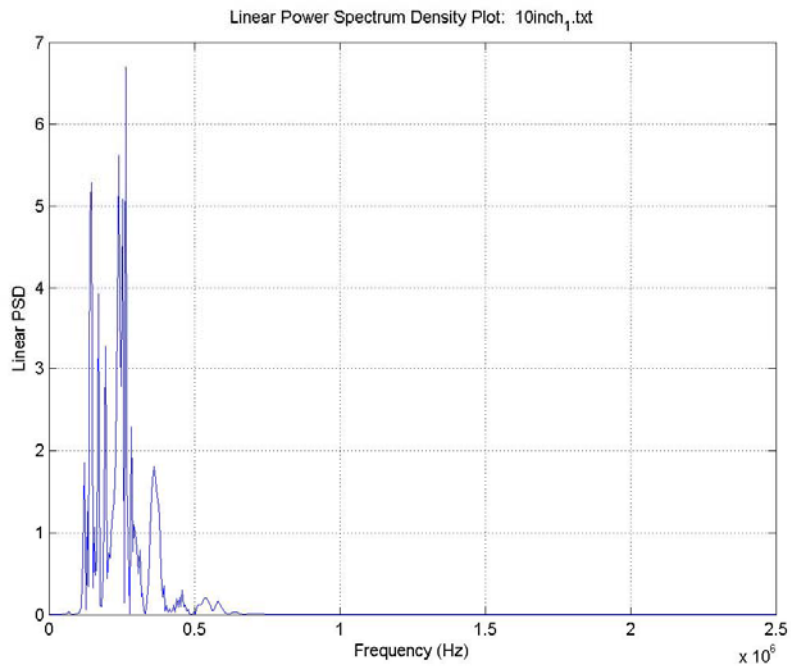


Figure 5.19: Linear frequency domain plot for the acquired signal.

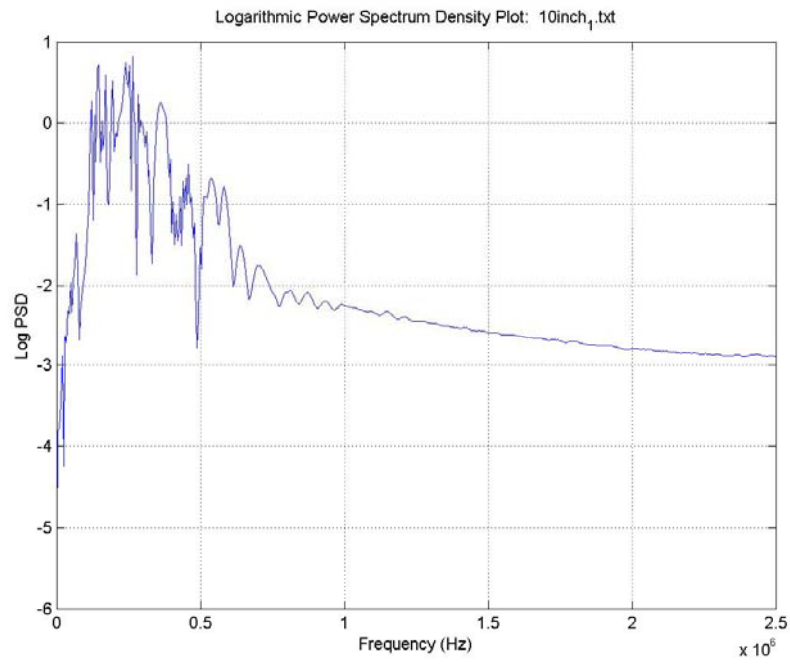


Figure 5.20: Logarithmic frequency domain plot for the acquired signal.

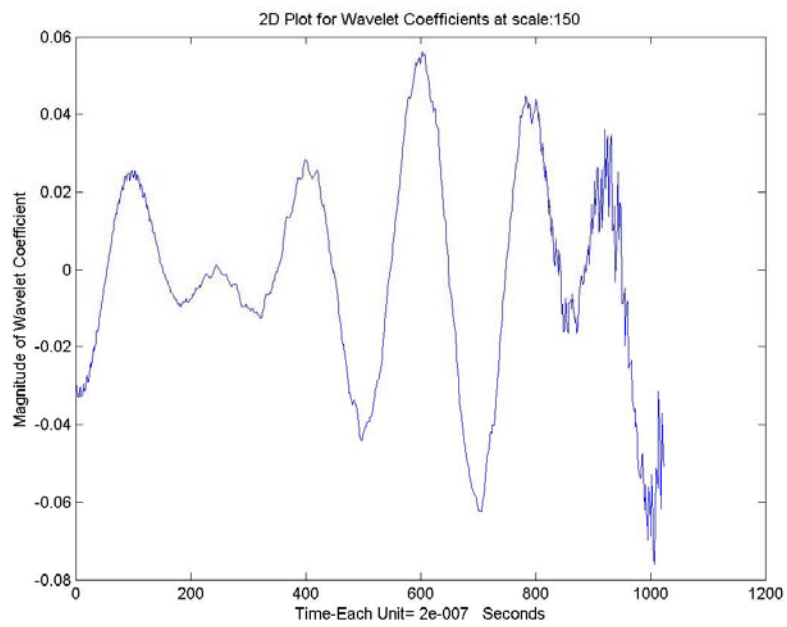


Figure 5.21: 2D plot of wavelet coefficients.

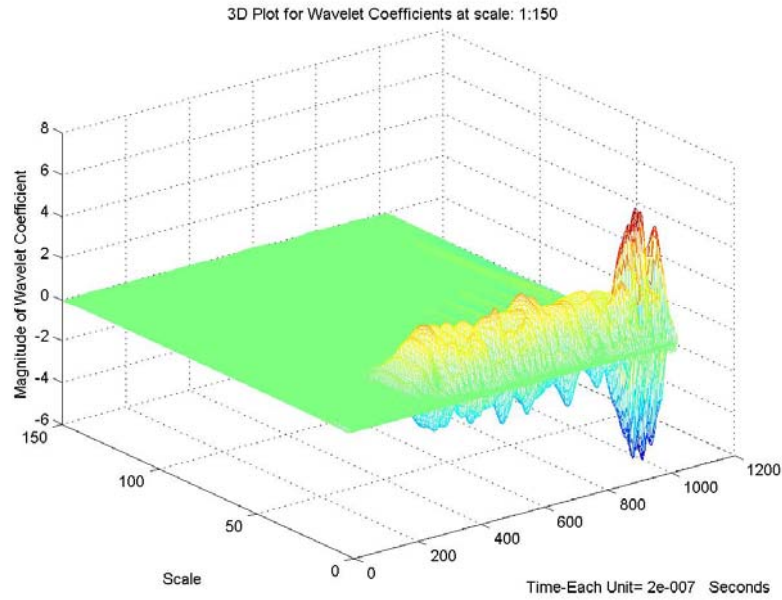


Figure 5.22: 3D plot of wavelet coefficient.

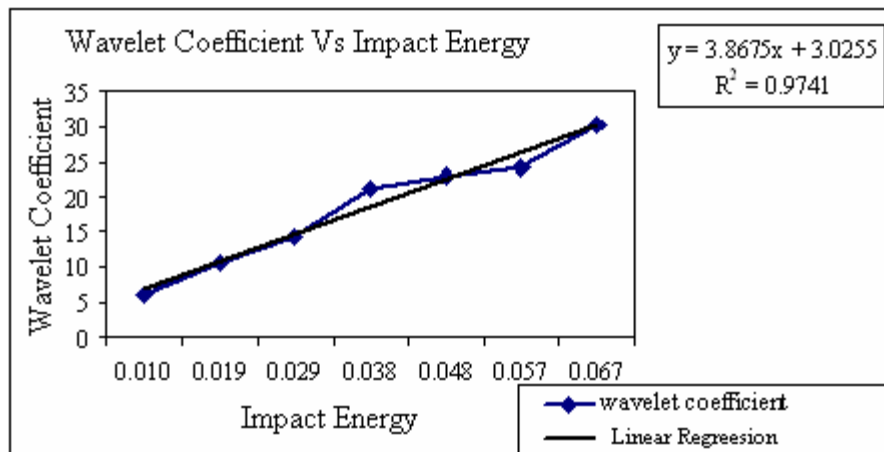


Figure 5.23: Variation of wavelet coefficient w.r.t. impact energy.

Secondly, 3-dimensional chart can also be such that speed of vehicle occupies number of columns, weight of vehicle occupies number of rows and the acoustic emission parameters (such as counts, energy) are filled in the table representing particular speed and weight in the vehicle. Also, a 3-D surface plot can be displayed with speed of vehicle on X-axis, weight of vehicle on Y-axis and acoustic emission parameters on Z-axis. A representative chart is shown in Table 5.6, where speed of vehicle is occupies number of columns, weight with in the vehicle occupies number of rows and acoustic emission parameters are the input to the table corresponding the particular speed and weight.

Table 5.6: 3-dimensional chart with acoustic emission parameters as input for particular speed and weight of vehicle

Speed Weight	5	10	15	20	25	30
1	Acoustic Emission Parameters corresponding the speed and weight of the vehicle					
2						
3						
4						
5						

The basic idea for developing this chart is that if we know the speed of the vehicle then the obtained acoustic emission parameter value can be correlated to the weight with in the vehicle. A test was conducted and the a chart was developed as shown in Table 5.7, which shows the variation of counts with the speed and weight with in the car and Table 5.8 shows the variation of signal energy with the speed and weight within the car.

Table 5.7: Variation of Counts with the speed and weight with in the car

Speed (mph) Mass (kg)*						
		10	15	20	25	30
1385	Car + 1 Passenger	395	354	567	889	885
1455	Car + 2 Passengers	316	485	452	452	815
1525	Car + 3 Passengers	475	722	730	499	889
1595	Car + 4 Passengers	742	639	562	1235	999
1665	Car + 5 Passengers	793	693	467	1259	1446

\* Represents the total mass of car, however only half the mass of car was used in experiment

Table 5.8: Variation of Energy with the speed and weight with in the car

Speed (mph) Mass (kg)*						
		10	15	20	25	30
1385	Car + 1 Passenger	141	207	740	480	1144
1455	Car + 2 Passengers	174	396	298	165	800
1525	Car + 3 Passengers	678	895	801	1219	1853
1595	Car + 4 Passengers	529	794	813	1145	2202
1665	Car + 5 Passengers	550	556	1827	1914	2182

\* Represents the total mass of car, however only half the mass of car was used in experiment

Figure 5.24 shows the surface plot for the number of counts as they vary with the speed and the weight with in the car when front wheel passes over the strip and Figure 5.25 shows a similar kind of surface plot for variation of signal energy with speed and weight with in the car when the front wheel passes over the strip. The car passes the strip such that half the axel passes over the strip.

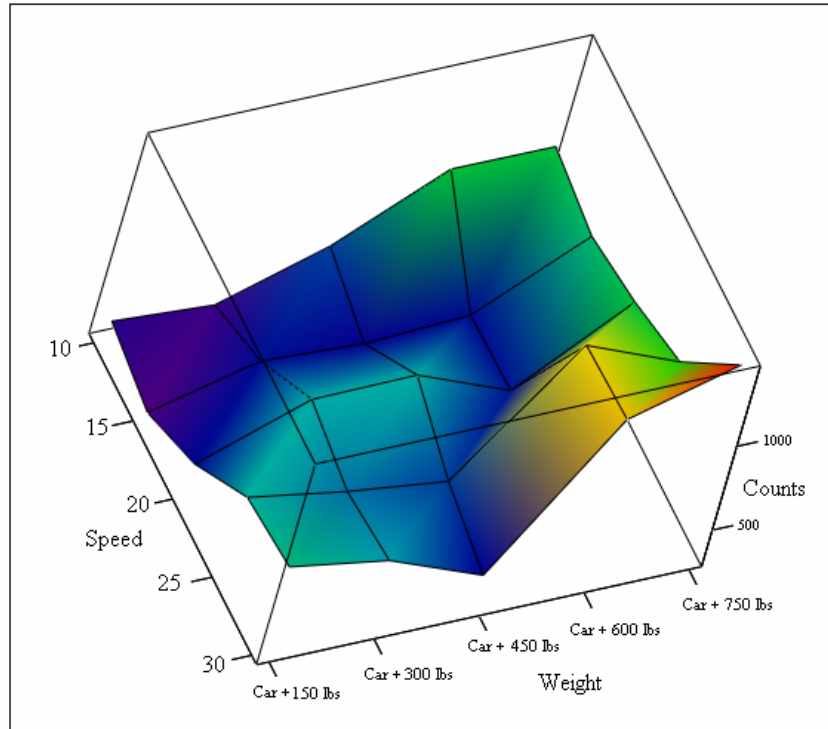


Figure 5.24: Surface plot for Counts with variation of speed and weight with in the Car

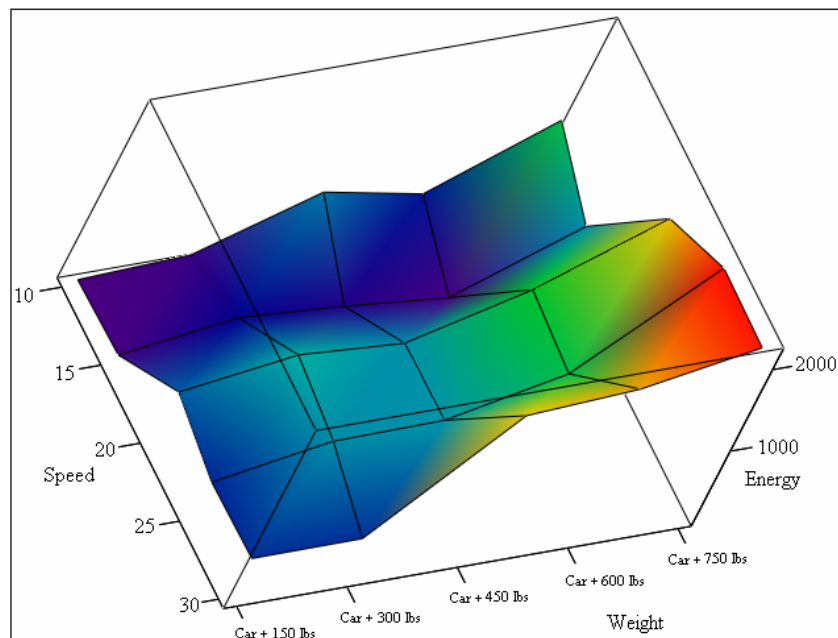


Figure 5.25: Surface plot for Energy with variation of speed and weight with in the Car

## CHAPTER SIX: CONCLUSIONS

A feasibility study on the use of acoustic emission for development of Weigh-in-Motion system was studied. The idea was to correlate the weight and speed of the vehicle with acoustic emission parameters.

Initial testing of plates for Kaiser Effect shows that the mechanism from which the acoustic signals generates is impact force and not any structural signals. Hence there is no significance of Kaiser Effect and we can use acoustic emission phenomenon for development of weigh-in-motion system. Speed of the car effect the number of signals being captured. A good polynomial correlation of second order was found between the AE parameters and the speed of vehicle. Absolute energy of the signal gives a better correlation among the AE parameters with the speed of vehicle. There is a linear regression between the variable impact force and acoustic emission parameters. Acoustic emission parameter increases with the increase in weight within the vehicle. A linear regression was found between the acoustic emission parameters and weight within the vehicle.

Further the possibility of using wavelet transform to determine the maximum wavelet coefficient and then correlating it with the weight of the vehicle is seen. An initial experimentation displayed that there is a linear correlation between the maximum wavelet coefficient and the impact energy.



## LIST OF REFERENCES

- 
- <sup>1</sup> 1996 Highway Statistics, Public Road Length 1996: Miles by Functional System, FHWA Office of Highway Information Management, 1996.
- <sup>2</sup> Truck Movements in America: Shipments From, To, Within, and Through States, TranStats, BTS/97-TS/1, Bureau of Transportation Statistics, 1997.
- <sup>3</sup> WIM Scale Calibration: A Vital Activity for LTPP Sites, Publication No. FHWA-RD-98-104, Federal Highway Administration, McLean, 1998.
- <sup>4</sup> Special Report 225: Truck Weight Limits: Issues and Options. p. 1, Transportation Research Board, National Research Council, Washington, D.C.,1990.
- <sup>5</sup> Special Report 225: Truck Weight Limits: Issues and Options. p. 135, Transportation Research Board, National Research Council, Washington, D.C.,1990.
- <sup>6</sup> Rich Quinley, Division of Traffic Operations, Caltrans, 1998.
- <sup>7</sup> McCall, B. and Vodrazka, W., Jr. (1997). States' successful practices weigh-in-motion handbook. Federal Highway Administration: Washington, DC.
- <sup>8</sup> Laurita, J., Sellner, G., and DuPlessis, D. (1994). Weigh-in-motion technology improves highway truck weight regulation. Public Works, June, 41-42
- <sup>9</sup> Weigh in motion technology comparisons, International Road Dynamics, January 2001
- <sup>10</sup> B. Taylor and A. Bergan, International Road Dynamics, Inc. The USE of Dual Weighing Elements (Double Threshold) to Improve the Accuracy of Weigh-in-Motion Systems, and the Effect of Accuracy on Weigh Station Sorting. Oregon

---

Department of Transportation, under Contract for the Port of Entry Advanced Sorting System (PASS) Project. November 1993.

<sup>11</sup> Bushman, R. and Pratt, A. (1998). Weigh in motion technology – economics and performance. North American Travel Monitoring, Exhibition and Conference, Charlotte, NC.

<sup>12</sup> PCI-2 Based AE system, User's Manual, Physical Acoustic Corporation

<sup>13</sup> H. Lamb, "On Waves in an Elastic Plate," Proc. R. Soc., A93 (1917) pp. 11 -128

<sup>14</sup> PAC Dispersion curve software developed by Physical Acoustic Corporation

<sup>15</sup> Acoustic Emission Signals in Thin Plates Produced by Impact Damage

William H. Prosser, Michael R. Gorman and Donald H. Humes

<sup>16</sup> Principles of Weight-in-Motion using Piezoelectric Axle Sensors